PMQ-VE: Progressive Multi-Frame Quantization for Video Enhancement

ZhanFeng Feng[1†], **Long Peng**[1†‡], **Xin Di**[1†], **Yong Guo**[2], **Wenbo Li**[3], **Yulun Zhang**[4], **Renjing Pei**[5*], **Yang Wang**[1,6*], **Yang Cao**[1*], **Zheng-Jun Zha**[1]

[1]USTC, [2]Max Planck Institute, [3]CUHK, [4]SJTU,
[5]Institute of Automation, Chinese Academy of Sciences, [6]Chang'an University

{xiaobigfeng, longp2001, dx9826}@mail.ustc.edu.cn, ywang120@chd.edu.cn

Abstract

Multi-frame video enhancement tasks aim to improve the spatial and temporal resolution and quality of video sequences by leveraging temporal information from multiple frames, which are widely used in streaming video processing, surveillance, and generation. Although numerous Transformer-based enhancement methods have achieved impressive performance, their computational and memory demands hinder deployment on edge devices. Quantization offers a practical solution by reducing the bit-width of weights and activations to improve efficiency. However, directly applying existing quantization methods to video enhancement tasks often leads to significant performance degradation and loss of fine details. This stems from two limitations: (a) inability to allocate varying representational capacity across frames, which results in suboptimal dynamic range adaptation; (b) over-reliance on full-precision teachers, which limits the learning of low-bit student models. To tackle these challenges, we propose a novel quantization method for video enhancement: Progressive Multi-Frame Quantization for Video Enhancement (PMQ-VE). This framework features a coarse-to-fine two-stage process: Backtracking-based Multi-Frame Quantization (BMFQ) and Progressive Multi-Teacher Distillation (PMTD). BMFQ utilizes a percentile-based initialization and iterative search with pruning and backtracking for robust clipping bounds. PMTD employs a progressive distillation strategy with both full-precision and multiple high-bit (INT) teachers to enhance low-bit models' capacity and quality. Extensive experiments demonstrate that our method outperforms existing approaches, achieving state-of-the-art performance across multiple tasks and benchmarks. The code will be made publicly available.

1 Introduction

Multi-frame video enhancement tasks aim to enhance the spatial and temporal resolution and quality of video sequences by exploiting temporal information from multiple frames. Among these, Video Frame Interpolation (VFI) [1, 20, 25, 39, 44, 46, 50, 53, 78–80, 86, 89], Video Super-Resolution (VSR) [3–6, 9, 22, 26], and Spatio-Temporal Video Super-Resolution (STVSR) [12, 17, 38, 66, 71, 72, 74, 87] are the most representative video enhancement methods. They are widely employed as post-processing and pre-processing techniques in social media platforms, gaming environments, and various video perception and generation tasks [4, 12]. Recent Transformer-based approaches for video enhancement exploit attention mechanisms to capture temporal dependencies across multiple frames, enabling substantial improvements in visual quality and structural fidelity. However, their high computational and memory demands remain a major obstacle for real-world deployment. Therefore, numerous

* Renjing Pei, Yang Wang and Yang Cao are the corresponding authors. † ZhanFeng Feng, Long Peng, and Xin Di contributed equally to this work. ‡ Long Peng is the project leader.

39th Conference on Neural Information Processing Systems (NeurIPS 2025).

studies have proposed various model quantization methods to compress the bit-width of weights and activations from 32 bits (FP32) to 8, 4, or 2 bits [19, 28, 40–42, 56, 57, 76]. This is a crucial step in practical deployment, reducing memory consumption and inference latency. For example, PAMS [28], a classic method in Post-Training Quantization (PTQ), introduces trainable scale parameters to dynamically learn the maximum value of the quantization range. Liu *et al.* propose 2DQuant [40], a dual-stage method for image super-resolution which designs a differentiated search strategy and uses knowledge distillation [16] to guide the learning of the quantization range. However, to the best of our knowledge, exploring model quantization in video enhancement remains largely uncharted. Directly applying existing quantization methods can lead to significant issues such as performance degradation and loss of fine details. Through observations and statistical experiments, we attribute these problems to two key limitations: (a) Video enhancement models need to aggregate texture and motion information from multiple frames, leading to inter-frame differential perception of information, manifesting as differentiated activation value distributions across frames as shown in Figure 2(a). However, traditional quantization methods fails to allocate inconsistent representational capacity to different frames, resulting in discrepancies in dynamic range across frames, as shown in Figure 2(b). This results in suboptimal utilization of sub-pixel spatial details, thereby limiting reconstruction performance. (b) Quantization inevitably reduces the representational capacity of the video model. Traditional methods overlook the capacity differences between the teacher (FP32) and student models (2bit, 4bit), relying solely on full-precision teachers for distillation. This makes it challenging for the student to learn high-quality mappings given its limited capacity, resulting in difficulty when directly quantizing a high-precision network into a low-precision one, as shown in Figure 1(a). To address these limitations, we propose a novel quantization framework: Progressive Multi-Frame Quantization for multi-frame Video Enhancement, called PMQ-VE. Specifically, PMQ-VE introduces a coarse-to-fine two-stage process, which includes Backtracking-based Multi-Frame Quantization (BMFQ) and Progressive Multi-Teacher Distillation (PMTD).

Coarse Stage: Backtracking-based Multi-Frame Quantization. Existing methods [40, 64] typically initialize quantization bounds using the global minimum and maximum values and symmetrically shrink them inward, ignoring inter-frame variations and the asymmetric nature of distributions. To address this, as illustrated in Figure 2(c), BMFQ assigns frame-specific clipping bounds to better match the heterogeneous activation statistics across video frames. BMFQ employs a percentile-based initialization to suppress outliers and performs a backtracking-based search with pruning and backtracking to search the bounds efficiently. This strategy enables accurate, adaptive quantization with negligible overhead,

Fine Stage: Progressive Multi-Teacher Distillation. In the fine stage, we introduce a Progressive Multi-Teacher Distillation framework to restore the model's representational capacity under low-bit quantization. Specifically, a full-precision teacher provides fine-grained feature supervision, while an intermediate 8/4-bit teacher offers quantization-aware guidance, helping the 4/2-bit student model learn stable and informative representations under low-bit constraints, bridging the gap between the quantized and full-precision models.

Extensive experiments on three representative video enhancement tasks—STVSR, VSR, and VFI—demonstrate that our method achieves state-of-the-art performance across multiple benchmarks for various tasks. Our method consistently outperforms existing methods, achieving the best performance on PSNR, SSIM across various bit-width settings, as shown in Figure 1(b-c). The contributions of this paper can be summarized as follows:

- To the best of our knowledge, we are the first to explore model quantization in multi-frame video enhancement tasks. We propose PMQ-VE, a novel per-frame coarse-to-fine quantization framework for multi-frame video enhancement models.
- In the coarse stage, we propose BMFQ to search quantization bounds via iterative backtracking with pruning, achieving efficient initialization. In the fine stage, we propose PMTD to leverage the knowledge of multi-level teachers to help a low-bit student model, enhancing its mapping quality and performance.
- Extensive experiments on three video enhancement tasks (STVSR, VSR, and VFI) demonstrate that our method achieves state-of-the-art results across various benchmarks under different low-bit quantization settings, highlighting the superiority and practicability of our approach.

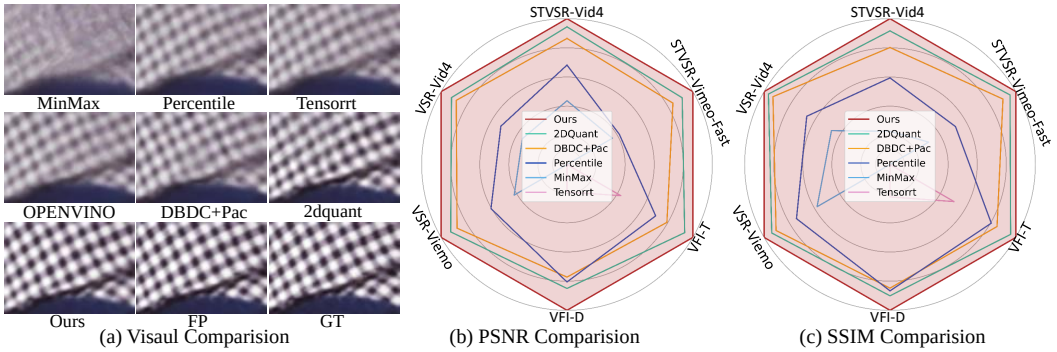

(a) Visaul Comparision (b) PSNR Comparision (c) SSIM Comparision

Figure 1: (a) Qualitative comparison of reconstructed frames using different quantization methods. Quantitative comparison of PSNR(b) and SSIM(c) improvements across three video enhancement tasks (STVSR, VFI, VSR). Our method consistently outperforms existing quantization approaches in both visual quality and quantitative metrics.

2 Related work

2.1 Video Enhancement

Video enhancement aims to exploit sub-pixel information from contextual frames to improve the quality and resolution of videos, which primarily includes video frame interpolation, video super-resolution, and spatio-temporal video super-resolution.

Video Frame Interpolation (VFI) targets generating the intermediate frames between given consecutive inputs. Early CNN-based methods [1, 20, 25, 44, 89] mainly rely on optical flow estimation or direct frame synthesis, but often suffer from limited receptive fields and poor handling of large motion. Therefore, Transformer-based approaches [39, 53, 86] have been proposed to model long-range dependencies, significantly improving the quality and detail of generated video.

Video Super-Resolution (VSR) aims to reconstruct high-resolution (HR) video from low-resolution (LR) inputs. Early VSR methods primarily used explicit optical flow alignment [3, 5, 63], dynamic filtering [26], deformable convolutions [67], and temporal attention mechanisms [30, 73]. With the increasing prominence of the Transformer's powerful representation capabilities, numerous Transformer-based VSR methods have been proposed, achieving progressive success. For example, PSRT [62] leverages a multi-frame self-attention mechanism to jointly process features from the current input frame and the propagated features. MIA [88] further boosts performance by leveraging masked intra-frame and inter-frame attention blocks to better use of previously enhanced features.

Spatio-Temporal Video Super-Resolution (STVSR) aims to simultaneously enhance spatial and temporal resolution, combining VSR and VFI, and presents greater challenges. Among the most representative real-time Transformer-based models is RSTT [12], which achieves state-of-the-art performance by constructing feature dictionaries from different levels of encoders and repeatedly querying them during the decoding stage.

Although powerful transformer-based models have demonstrated superiority in enhancing spatial resolution and perceptual quality, their high computational cost hinders practical deployment. This paper is the first to propose an efficient model compression method specifically for video enhancement to facilitate its deployment.

2.2 Model Quantization

Model quantization aims to reduce the model's bit-width, from the Float 32-bit used in training to int 8, 4, or 2-bit for deployment, significantly reducing computational and memory costs and is widely applied in various fields such as LLM and VLM, etc. Quantization is divided into post-training quantization (PTQ) and Quantization-Aware Training (QAT). QAT, requiring simultaneous training and quantization, demands significant resources and data. PTQ, applied after pre-training, is more efficient and thus receives greater research focus. Early PTQ methods focused on minimizing quantization error using efficient calibration techniques [34, 76]. Recent approaches, such as AdaRound [70] and BRECQ [33], refine weight quantization by minimizing layer-wise output discrepancies. Additionally, robustness-oriented methods like NoisyQuant [42], OASQ [47], and ERQ [85] enhance PTQ performance by mitigating quantization noise, suppressing outliers, or optimizing error-aware objectives.

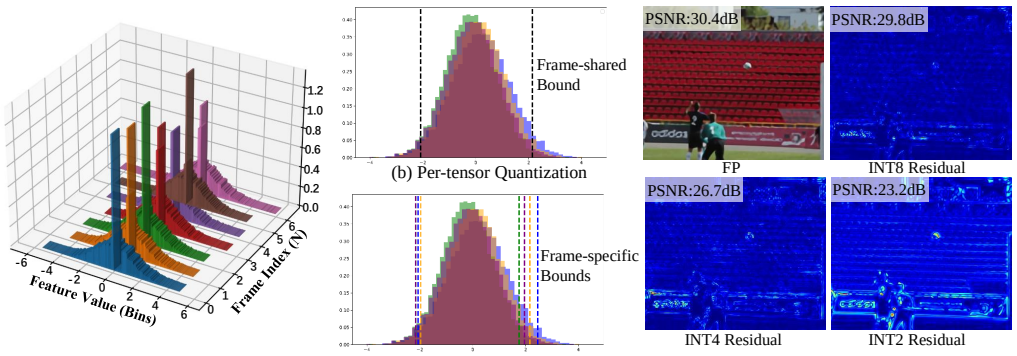

(a) Variation of Feature Distributions across Frames (c) Per-frame Quantization (d) Residuals under different bit widths

Figure 2: Finding and Motivation. (a) In multi-frame video enhancement, activation distributions vary significantly across frames. Traditional per-tensor quantization (b) fails to dynamically adjust quantization bounds for these variations, but our method (c) achieves this dynamic adjustment. (d) We calculated PSNR and residual maps for FP, INT8, INT4, and INT2 with respect to GT. The significant gap between low-bit (INT2/4) and full-precision (FP) model suggests that low-bit struggles to learn directly from FP. This inspired us to use multiple teacher models for supervision.

However, existing work mainly addresses high-level vision/language tasks and is often unsuitable for pixel-level image/video enhancement, which is sensitive to quantization errors due to its reliance on fine-grained features. Recent research has thus started exploring quantization for pixel-level image enhancement and super-resolution [7, 8, 37, 61, 82]. For example, DBDC+Pac [64] introduces a PTQ framework for image super-resolution, combining calibration techniques with knowledge distillation from a full-precision teacher model. Similarly, 2DQuant [40] targets SwinIR [35] by proposing a one-sided search algorithm to quantize sensitive activations, such as post-softmax and post-GELU [18] layers. These methods often overlook inter-frame differences in multi-frame video enhancement, limiting detail representation and resulting in blurred images.

3 Methodology

3.1 Problem Formulation

Model quantization aims to learn appropriate clipping ranges [40, 64, 76] for each tensor (e.g., weights or activations) in order to minimize the discrepancy between the outputs of the full-precision model and the quantized model. Following previous work [40, 41, 64], we use fake quantization [24] to simulate the quantization process. Given a pre-learned clipping range $[lb, ub]$ for a tensor x, the quantization and dequantization process is defined as follows:

$$x_{\text{clip}} = \text{clamp}(x, lb, ub) = \min(\max(x, lb), ub), \tag{1}$$

$$x_{\text{int}} = \text{round}\left(\frac{x_{\text{clip}} - lb}{\Delta}\right), \quad \Delta = \frac{ub - lb}{2^N - 1}, \quad \hat{x} = x_{\text{int}} \cdot \Delta + lb, \tag{2}$$

Where x_{clip} is the clipped tensor, $x_{\text{int}} \in \{0, 1, \ldots, 2^N - 1\}$ is the quantized integer, Δ is the quantization step size, and $\hat{x}$ is the dequantized approximation of the original value. Linear and MatMul layers are the most computationally intensive components in Transformer-based architectures. We follow existing work [40, 42] to focus quantization on these modules. Since the quantization function is non-differentiable due to rounding, we also adopt the Straight-Through Estimator (STE) [10] during training to approximate gradients and enable end-to-end optimization under quantized settings. More details are in the **Appendix A**.

3.2 Observations and Motivation

Observation 1: Inability to allocate varying representational capacity across frames. Previous studies have thoroughly examined the statistical properties of activations in Transformer-based architectures, uncovering long-tailed distributions and a mix of symmetric and asymmetric behaviors across layers [34, 40, 49, 76, 85]. However, these analyses are largely confined to single-frame scenarios. In the context of quantizing multi-frame video enhancement networks, it is essential

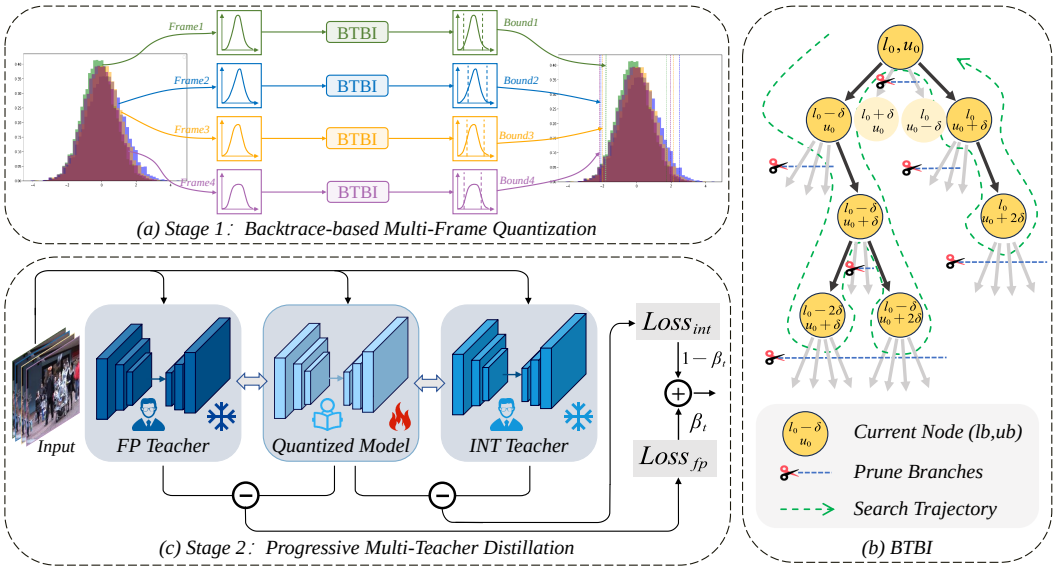

Figure 3: The overall framework of our proposed method.

to preserve the capability of the full-precision network to effectively integrate inter-frame texture information and motion cues—a challenge that vanilla methods fail to address.

Our analysis reveals that multi-frame networks perceive and process each frame in the input tensor differently. As shown in Figure 2(a), we collect per-frame activation statistics and observe significant disparities in activation distributions across frames. In particular, the value ranges (i.e., the minimum and maximum activation values) vary considerably, indicating that the network allocates representational capacity unevenly across frames. These differences are influenced by the model's frame-dependent attention dynamics. In particular, the network assigns different attention weights to each frame, resulting in varied activation distributions. Consequently, applying existing Transformer quantization methods [34, 40, 49, 76, 85], which typically assume a unified activation distribution, can be suboptimal for multi-frame models. Such methods overlook inter-frame variation, leading to inefficient quantization and increased error, ultimately degrading the quality of the output.

Observation 2: Over-reliance on full-precision teachers limits low-bit model learning. Low-bit quantization inevitably reduces the representational capacity of models, which brings significant challenges to multi-frame video enhancement tasks. Under low-bit quantization, both activation values and network precision degrade noticeably, making it difficult to maintain the clear motion trajectories and rich texture details required for these tasks. As shown in Figure 2(c), directly quantizing the network to 4-bit/2-bit and applying it without adaptation leads to severe artifacts and motion blur. The main reason for this degradation lies in the large quantization errors introduced when networks are directly quantized to low-bit precision. Furthermore, traditional methods often overlook the capacity gap between the teacher model (FP32) and the student model (e.g., 4-bit or 2-bit), relying solely on full-precision teachers for knowledge distillation [16, 40, 64]. This makes it difficult for the student model to learn high-quality mappings within its limited capacity, further increasing the challenge of achieving satisfactory performance under low-bit constraints.

3.3 Proposed Method

Based on the above observations, we propose a two-stage quantization framework. The coarse stage uses Backtracking-based Multi-Frame Quantization (BMFQ) to initialize asymmetric bounds efficiently. The fine stage applies Progressive Multi-Teacher Distillation (PMTD) to refine bounds.

3.3.1 Backtracking-based Multi-Frame Quantization

Motivated by Observation 1, we adopt a per-frame quantization strategy to handle frame-wise variations in activation distributions and representational capacity. Given a multi-frame activation tensor $X \in \mathbb{R}^{N\times C\times H\times W}$, where N denotes the number of frames, we independently search the clipping bounds for each frame $X_i = X[i,:,:,:]$, yielding frame-specific clipping parameters (lb_i, ub_i) for $i = 1, \ldots, N$. This strategy enables the quantizer to adapt to frame-specific activation

statistics, thereby improving quantization accuracy.

To robustly estimate the clipping bounds during the coarse stage, we formulate the selection of (lb_i, ub_i) as a constrained optimization problem that minimizes quantization-induced distortion over a percentile-based search space S_i derived from the empirical distribution of X_i:

$$(lb_i^*, ub_i^*) = \underset{(lb,ub)\in S_i}{\arg\min}\ \mathbb{E}_{x\sim X_i}\left[(x - Q_{lb,ub}(x))^2\right], \tag{3}$$

Here, $Q_{lb,ub}(\cdot)$ denotes a uniform quantizer [43] with clipping range $[lb, ub]$. To mitigate the influence of outliers, we constrain the search space S_i using percentiles: $lb \in [p_{0.1}(X_i), p_{10}(X_i)]$, $ub \in [p_{90}(X_i), p_{99.9}(X_i)]$, where $p_k(X)$ denotes the k-th percentile of the tensor X. To efficiently solve the optimization problem in Eq. (3), we introduce a Backtracking-based Bound Initialization (BTBI) algorithm. Starting from an initial estimate derived from the percentiles of X_i, the algorithm recursively explores candidate bounds by adjusting lb_i and ub_i within the search space S_i. At each step, it evaluates the quantization error and updates the optimal bounds if a better configuration is found. To avoid redundant searches, previously visited bounds are skipped. The algorithm backtracks to explore alternative adjustments when no further improvement is achieved, terminating when all candidates are evaluated or a convergence threshold is met. In contrast to traditional methods that uniformly shrink bounds [40] or adjust them sequentially [64], BTBI is less sensitive to outliers and explores a richer set of candidate configurations. By combining frame-wise adaptation with recursive backtracking search, BTBI robustly converges to optimal clipping parameters for each frame. To enhance understanding, we provide a detailed algorithm of our BTBI in Algorithm 1.

Algorithm 1 Backtracking-based Bound Initialization (BTBI) pipeline

Input: X, step sizes ΔL, ΔU, threshold ε
Output: Optimal bounds lb^*, ub^*
$visited \leftarrow \emptyset$, $error_{\min} \leftarrow \infty$
Function `Backtrack`(lb, ub)**:**
  if $(lb, ub) \in$ *visited or out-of-range* **then**
    return
  $visited \leftarrow visited \cup \{(lb, ub)\}$
  $X_q \leftarrow$ Quantize X using (lb, ub)
  $err \leftarrow \|X - X_q\|_2$
  if $err > error_{\min} + \varepsilon$ **then**
    return
  if $err < error_{\min}$ **then**
    $error_{\min} \leftarrow err$
    $lb^* \leftarrow lb$
    $ub^* \leftarrow ub$
  foreach $(\delta_l, \delta_u) \in \{\pm\Delta L, \pm\Delta U\}$ **do**
    `Backtrack`$(lb + \delta_l, ub + \delta_u)$
`Backtrack`(lb_0, ub_0)
return lb^*, ub^*

3.3.2 Progressive Multi-Teacher Distillation

As revealed by Observation 2, training accurate quantized models under extremely low-bit settings (e.g., 4-bit or 2-bit) remains challenging due to limited capacity and optimization instability. To address this, we propose Progressive Multi-Teacher Distillation (PMTD), a hierarchical distillation framework that leverages both high-bit and full-precision teachers to facilitate low-bit training. Instead of directly distilling knowledge from a full-precision (FP) teacher to a low-bit student, which often suffers from large representational gaps, PMTD introduces intermediate-bit teacher models (e.g., 8-bit) between the full-precision (FP) teacher and the low-bit student. These intermediate teachers serve as quantization-aware approximations of the FP model, providing smoother supervision and easing the optimization process. This hierarchical approach effectively bridges the representational gap between student and teacher models, ensuring more stable training dynamics and improved performance under extreme quantization constraints. Specifically, to train a 4-bit quantized model, PMTD first uses the full-precision model as a teacher to train an 8-bit model. When training the 4-bit model, both the full-precision network and the 8-bit network are used as teacher models, as illustrated in Figure 3(c). The distillation process is formally defined by the following loss function:

$$\mathcal{L}_{\text{PMTD}} = (\mathcal{L}_{\text{INT}} + \alpha(t) \cdot \mathcal{L}_{\text{FP}})/(1 + \alpha(t)), \tag{4}$$

where $\mathcal{L}_{\text{INT}}$ denotes the total loss from intermediate-bit teachers (e.g., 8-bit), and $\mathcal{L}_{\text{FP}}$ represents the loss from the full-precision teacher. The balancing coefficient $\alpha(t)$ linearly increases over time and is defined as $\alpha(t) = \min\left(1, \frac{t}{T_{\text{warmup}}}\right)$, where T_{warmup} is a hyperparameter controlling the warm-up duration. Each teacher-specific loss consists of two components: an output-level reconstruction loss

Table 1: Quantitative comparison of different methods on four STVSR benchmarks. The best and the second best results are in **bold** and bold.

Method	Bit	Vid4		Vimeo-Fast		Vimeo-Medium		Vimeo-Slow	
		PSNR↑	SSIM↑	PSNR↑	SSIM↑	PSNR↑	SSIM↑	PSNR↑	SSIM↑
RSTT-S [12]	32/32	26.29	0.7941	36.58	0.9381	35.43	0.9358	33.30	0.9123
Trilinear	32/32	22.90	0.5883	29.45	0.8019	29.16	0.8351	28.21	0.8091
OpenVINO [15]	2/2	18.24	0.3151	23.39	0.6103	23.60	0.6227	23.87	0.6242
TensorRT [65]	2/2	20.31	0.5118	23.41	0.6106	23.61	0.6236	23.88	0.6283
SNPE [21]	2/2	15.22	0.2378	23.40	0.6106	23.61	0.6241	23.88	0.6281
Percentile [29]	2/2	12.67	0.1349	15.27	0.2274	14.80	0.2165	14.67	0.2156
MinMax [23]	2/2	10.34	0.0138	10.52	0.0266	10.48	0.0289	10.45	0.0303
NoisyQuant [42]	2/2	12.06	0.1028	12.50	0.1669	11.81	0.1465	11.49	0.1508
DBDC+Pac [64]	2/2	22.64	0.5695	28.94	0.8254	28.87	0.8214	27.86	0.7905
2DQuant [40]	2/2	22.91	0.5883	29.38	0.8315	29.14	0.8330	28.18	0.8086
Ours	2/2	**23.48**	**0.6252**	**30.33**	**0.8424**	**30.19**	**0.8523**	**29.14**	**0.8316**
OpenVINO [15]	4/4	18.84	0.4591	21.82	0.6372	21.63	0.6315	18.84	0.4591
TensorRT [65]	4/4	18.63	0.4578	21.74	0.6019	21.70	0.6324	18.63	0.4578
SNPE [21]	4/4	17.84	0.3977	21.64	0.6018	21.56	0.6301	18.76	0.4584
Percentile [29]	4/4	23.26	0.6314	27.12	0.7664	27.16	0.7709	26.58	0.7531
MinMax [23]	4/4	21.60	0.5242	26.41	0.6990	25.94	0.7059	25.44	0.6957
NoisyQuant [42]	4/4	24.26	0.6905	31.22	0.8719	30.64	0.8705	29.61	0.8462
DBDC+Pac [64]	4/4	24.50	0.6923	32.64	0.8857	32.06	0.8866	30.64	0.8643
2DQuant [40]	4/4	25.04	0.7256	33.59	0.9035	32.83	0.9009	31.21	0.8766
Ours	4/4	**25.42**	**0.7501**	**34.69**	**0.9181**	**33.74**	**0.9150**	**31.94**	**0.8903**

and an intermediate feature-matching loss:

$$\mathcal{L}_{\text{INT}} = \sum_{k=1}^{K} \left(\mathcal{L}_{\text{rec}}^{(k)} + \lambda \cdot \mathcal{L}_{\text{feat}}^{(k)} \right), \tag{5}$$

$$\mathcal{L}_{\text{FP}} = \mathcal{L}_{\text{rec}}^{\text{FP}} + \lambda \cdot \mathcal{L}_{\text{feat}}^{\text{FP}}, \tag{6}$$

where K is the number of intermediate-bit teachers (e.g., $K = 2$ when using 4-bit and 8-bit teachers), $\mathcal{L}_{\text{rec}}$ is the ℓ_1 loss [36] between the student and teacher outputs, and $\mathcal{L}_{\text{feat}}$ is the mean squared error (MSE) [2] between selected intermediate feature representations. The balancing coefficient λ is set to 5 to emphasize the importance of internal consistency. By gradually transitioning supervision from intermediate-bit to full-precision teachers, PMTD effectively reduces the training difficulty of low-bit models, mitigates quantization errors, and offers a more stable optimization path. This hierarchical approach ensures high-quality quantized outputs, even under extreme quantization constraints.

4 Experiment and Analysis

4.1 Experiment Setting

Datasets and backbone. We evaluate our method on three representative video enhancement tasks: Space-Time Video Super-Resolution (STVSR), Video Super-Resolution (VSR), and Video Frame Interpolation (VFI). For each task, we select state-of-the-art and popular methods as backbones: RSTT [12] for STVSR, MIA [88] for VSR, and EMA-VFI [86] for VFI. The Vimeo-90K [74] dataset is used for training across all tasks, with Vid4 [38] and the Vimeo-90K test set serving as evaluation benchmarks. More details of data preparation and setting are provided in the supplementary material.
Evaluation metrics. We use PSNR and SSIM [68] as evaluation metrics, computed on the luminance (Y) channel of the YCbCr color space. To further evaluate perception-oriented metrics, LPIPS [81] and NIQE [48] are used to assess the perceptual quality of videos.
Implementation details. We adopt the Adam optimizer [27] with an initial learning rate of 2×10^{-4}

Table 2: Quantitative comparison of different methods on two VFI EMA-VFI variants ([T] and [D]), evaluated on the Vimeo90K benchmark under 4-bit.

Method	Bit	EMA-VFI [T] [78]				EMA-VFI [D] [86]			
		PSNR↑	SSIM↑	LPIPS↓	NIQE↓	PSNR↑	SSIM↑	LPIPS↓	NIQE↓
Baseline	32/32	29.41	0.9279	0.086	6.736	30.29	0.9418	0.078	6.545
OpenVINO [15]	4/4	26.03	0.8703	0.222	8.022	25.38	0.8579	0.257	8.2784
TensorRT [65]	4/4	25.33	0.8551	0.268	8.582	25.21	0.8537	0.269	8.4035
SNPE [21]	4/4	25.49	0.8581	0.259	8.500	25.83	0.8683	0.236	8.0399
Percentile [29]	4/4	26.82	0.8919	0.185	7.765	28.54	0.9198	0.132	7.0667
MinMax [23]	4/4	23.03	0.7918	0.389	9.475	24.19	0.8309	0.313	8.5153
DBDC+Pac[64]	4/4	27.30	0.8976	0.171	7.545	28.36	0.9179	0.134	7.1221
2DQuant [40]	4/4	28.06	0.9110	0.152	7.494	28.78	0.9233	0.120	6.9884
Ours	4/4	**28.41**	**0.9162**	**0.136**	**7.361**	**29.59**	**0.9335**	**0.101**	**6.7881**

Table 3: Quantitative comparison of different methods on two VSR benchmarks under 4-bit.

Benchmark	Metric	Baseline: MIA [88]	TensorRT [65]	SNPE [21]	Percentile [29]	MinMax [23]	DBDC +Pac [64]	2DQuant [40]	Ours
Vimeo90K	PSNR↑	38.32	31.81	32.42	35.15	34.13	36.64	36.92	**37.34**
	SSIM↑	0.9532	0.8612	0.8805	0.9262	0.9119	0.9404	0.9434	**0.9487**
Vid4	PSNR↑	28.20	24.48	24.22	26.14	25.60	27.26	27.38	**27.64**
	SSIM↑	0.8507	0.6758	0.6877	0.7805	0.7494	0.8230	0.8287	**0.8341**

and apply Cosine Annealing [45] over 20,000 iterations. The batch size is set to 8 and 2 per GPU during the initialization and distillation-based fine-tuning phases, respectively. Random cropping, rotations, and flipping are applied to enhance training robustness. All experiments are implemented in Python with PyTorch [54] and conducted on 8 NVIDIA V100 GPUs.

4.2 Quantitative Results

Table 1 presents quantitative comparisons of various methods under 2/2, 4/4, bit-width across four STVSR benchmarks. Traditional quantization approaches, such as OpenVINO [15] and TensorRT [65], face challenges in pixel-level video enhancement, resulting in model performance scores of only 18.24dB and 20.31dB on Vid4 at 2-bit quantization. Although DBDC+Pac [64] and 2DQuant [40] are tailored for low-level vision tasks with enhanced sharpness awareness, which somewhat mitigates the performance drop due to quantization, they still lag behind our proposed method. This is primarily due to their limitations in managing multi-frame distribution differences and detail enhancement. Our method achieves the best performance across all scenarios and benchmarks, notably surpassing existing methods by nearly 1 dB on the Vimeo benchmark, underscoring the effectiveness of our approach. In a similar manner, our method demonstrates superior performance across all benchmarks and bit-width configurations for both Video Super-Resolution (VSR) and Video Frame Interpolation (VFI) tasks. As detailed in Tables 2 and 3, our approach exemplifies remarkable generalization capabilities, consistently outperforming existing methods in all benchmarks and bits. More results on additional bit-width settings and benchmarks can be found in **Appendix E**.

4.3 Qualitative Results

To verify the visual quality, we present the visual comparisons of different PTQ methods applied to STVSR, VSR and VFI tasks under 4-bit quantization, as shown in Figure 4. Traditional methods such as MinMax [23] and Percentile [29] exhibit noticeable artifacts, while other methods like DBDC+Pac [64] and 2dquant [40] suffer from detail blurring issues, particularly in complex scenes. However, our proposed method consistently produces sharper edges and more faithful textures that are visually closer to the full-precision outputs. In more challenging cases, such as the Vimeo-Fast dataset where motion and fine details coexist, our proposed method better preserves structural information

Figure 4: Visual comparisons under 4-bit quantization for three video enhancement tasks: from top to bottom are STVSR, VSR, and VFI tasks. More results are provided in Appendix F.

and avoids common artifacts. This highlights the visual superiority of our approach. More visual effects and comparisons with user studies will be presented in the **Appendix F**.

4.4 Ablation Studies

To validate the effectiveness of the proposed core idea, we design several ablation experiments to explore the multi-teacher distillation strategy the frame-wise quantization strategy. Specifically, we conduct experiments on STVSR in a 2-bit compression setting, removing these core modules one by one, with results shown in Table 6. It is seen that the baseline without any core ideas achieves only 12.67dB. By introducing the frame-wise quantization strategy, the network perceives differences between frames, improving performance. Furthermore, the BMFQ helps the network adaptively learn clipping ranges for each frame, boosting model performance to 27.56dB. Finally, with the introduction of the multi-teacher distillation strategy, the low-bit network learns prior knowledge from different teachers, further improving model performance despite limited capacity. This validates the effectiveness of the proposed core modules. **More ablation studies are presented in the Appendix H.**

Table 4: Ablation studies.

Per-Frame Quantization	BMFQ	PMTD	PSNR↑
✗	✗	✗	12.67
✓	✗	✗	19.64
✓	✓	✗	27.56
✓	✓	✓	30.33

5 Conclusion

We introduced a novel coarse-to-fine PMQ-VE, addressing key challenges in quantizing multi-frame video enhancement models. BMFQ is proposed to establish robust quantization bounds through a percentile-based initialization and backtracking search, ensuring efficient quantization across frames. PMTD enhances the quality of low-bit models by utilizing a progressive distillation strategy with both full-precision and quantized teachers, bridging the gap between high-precision and low-bit models. Experiments on STVSR, VSR, and VFI tasks show that our PMQ-VE achieves state-of-the-art performance and visually pleasing results.

Limitation and Future Work: Although our PMQ-VE has achieved promising results on Transformer-based video enhancement methods, more diffusion-based Transformer (DiT) methods can be tested. In the future, we plan to extend our method to more video enhancement tasks and models to facilitate the deployment of video models in the community.

Acknowledgments

This work was supported by the Natural Science Foundation of China under Grants 62225207,62436008 and 62206262. The AI-driven experiments, simulations and model training were performed on the robotic AI-Scientist platform of Chinese Academy of Sciences.

References

[1] Wenbo Bao, Wei-Sheng Lai, Chao Ma, Xiaoyun Zhang, Zhiyong Gao, and Ming-Hsuan Yang. Depth-aware video frame interpolation. In *Proceedings of the IEEE/CVF conference on computer vision and pattern recognition*, pages 3703–3712, 2019.

[2] Eric Bauer and Ron Kohavi. An empirical comparison of voting classification algorithms: Bagging, boosting, and variants. *Machine learning*, 36:105–139, 1999.

[3] Jose Caballero, Christian Ledig, Andrew Aitken, Alejandro Acosta, Johannes Totz, Zehan Wang, and Wenzhe Shi. Real-time video super-resolution with spatio-temporal networks and motion compensation. In *Proceedings of the IEEE conference on computer vision and pattern recognition*, pages 4778–4787, 2017.

[4] Jiezhang Cao, Yawei Li, Kai Zhang, and Luc Van Gool. Video super-resolution transformer. *arXiv preprint arXiv:2106.06847*, 2021.

[5] Kelvin CK Chan, Xintao Wang, Ke Yu, Chao Dong, and Chen Change Loy. Basicvsr: The search for essential components in video super-resolution and beyond. In *Proceedings of the IEEE/CVF conference on computer vision and pattern recognition*, pages 4947–4956, 2021.

[6] Kelvin CK Chan, Shangchen Zhou, Xiangyu Xu, and Chen Change Loy. Basicvsr++: Improving video super-resolution with enhanced propagation and alignment. In *Proceedings of the IEEE/CVF conference on computer vision and pattern recognition*, pages 5972–5981, 2022.

[7] Yujie Chen, Haotong Qin, Zhang Zhang, Michelo Magno, Luca Benini, and Yawei Li. Q-mambair: Accurate quantized mamba for efficient image restoration. *arXiv preprint arXiv:2503.21970*, 2025.

[8] Zheng Chen, Haotong Qin, Yong Guo, Xiongfei Su, Xin Yuan, Linghe Kong, and Yulun Zhang. Binarized diffusion model for image super-resolution. *arXiv preprint arXiv:2406.05723*, 2024.

[9] Myungsub Choi, Heewon Kim, Bohyung Han, Ning Xu, and Kyoung Mu Lee. Channel attention is all you need for video frame interpolation. In *Proceedings of the AAAI conference on artificial intelligence*, volume 34, pages 10663–10671, 2020.

[10] Matthieu Courbariaux, Itay Hubara, Daniel Soudry, Ran El-Yaniv, and Yoshua Bengio. Binarized neural networks: Training deep neural networks with weights and activations constrained to+ 1 or-1. *arXiv preprint arXiv:1602.02830*, 2016.

[11] Xin Di, Long Peng, Peizhe Xia, Wenbo Li, Renjing Pei, Yang Cao, Yang Wang, and Zheng-Jun Zha. Qmambabsr: Burst image super-resolution with query state space model. In *Proceedings of the Computer Vision and Pattern Recognition Conference*, pages 23080–23090, 2025.

[12] Zhicheng Geng, Luming Liang, Tianyu Ding, and Ilya Zharkov. Rstt: Real-time spatial temporal transformer for space-time video super-resolution. In *Proceedings of the IEEE/CVF conference on computer vision and pattern recognition*, pages 17441–17451, 2022.

[13] Yunpeng Gong, Liqing Huang, and Lifei Chen. Person re-identification method based on color attack and joint defence. In *CVPR, 2022*, pages 4313–4322, 2022.

[14] Yunpeng Gong, Chuangliang Zhang, Yongjie Hou, Lifei Chen, and Min Jiang. Beyond dropout: Robust convolutional neural networks based on local feature masking. In *2024 International Joint Conference on Neural Networks (IJCNN)*, pages 1–8. IEEE, 2024.

[15] Yury Gorbachev, Mikhail Fedorov, Iliya Slavutin, Artyom Tugarev, Marat Fatekhov, and Yaroslav Tarkan. Openvino deep learning workbench: Comprehensive analysis and tuning of neural networks inference. In *Proceedings of the IEEE/CVF International Conference on Computer Vision Workshops*, pages 0–0, 2019.

[16] Jianping Gou, Baosheng Yu, Stephen J Maybank, and Dacheng Tao. Knowledge distillation: A survey. *International Journal of Computer Vision*, 129(6):1789–1819, 2021.

[17] Muhammad Haris, Greg Shakhnarovich, and Norimichi Ukita. Space-time-aware multi-resolution video enhancement. In *Proceedings of the IEEE/CVF conference on computer vision and pattern recognition*, pages 2859–2868, 2020.

[18] Dan Hendrycks and Kevin Gimpel. Gaussian error linear units (gelus). *arXiv preprint arXiv:1606.08415*, 2016.

[19] Cheeun Hong, Heewon Kim, Sungyong Baik, Junghun Oh, and Kyoung Mu Lee. Daq: Channel-wise distribution-aware quantization for deep image super-resolution networks. In *Proceedings of the IEEE/CVF Winter Conference on Applications of Computer Vision*, pages 2675–2684, 2022.

[20] Zhewei Huang, Tianyuan Zhang, Wen Heng, Boxin Shi, and Shuchang Zhou. Real-time intermediate flow estimation for video frame interpolation. In *European Conference on Computer Vision*, pages 624–642. Springer, 2022.

[21] Andrey Ignatov, Radu Timofte, William Chou, Ke Wang, Max Wu, Tim Hartley, and Luc Van Gool. Ai benchmark: Running deep neural networks on android smartphones. In *Proceedings of the European Conference on Computer Vision (ECCV) Workshops*, pages 0–0, 2018.

[22] Takashi Isobe, Xu Jia, Shuhang Gu, Songjiang Li, Shengjin Wang, and Qi Tian. Video super-resolution with recurrent structure-detail network. In *Computer Vision–ECCV 2020: 16th European Conference, Glasgow, UK, August 23–28, 2020, Proceedings, Part XII 16*, pages 645–660. Springer, 2020.

[23] Benoit Jacob, Skirmantas Kligys, Bo Chen, Menglong Zhu, Matthew Tang, Andrew Howard, Hartwig Adam, and Dmitry Kalenichenko. Quantization and training of neural networks for efficient integer-arithmetic-only inference. In *Proceedings of the IEEE conference on computer vision and pattern recognition*, pages 2704–2713, 2018.

[24] Benoit Jacob, Skirmantas Kligys, Bo Chen, Menglong Zhu, Matthew Tang, Andrew Howard, Hartwig Adam, and Dmitry Kalenichenko. Quantization and training of neural networks for efficient integer-arithmetic-only inference. In *Proceedings of the IEEE conference on computer vision and pattern recognition*, pages 2704–2713, 2018.

[25] Zhaoyang Jia, Yan Lu, and Houqiang Li. Neighbor correspondence matching for flow-based video frame synthesis. In *Proceedings of the 30th ACM International Conference on Multimedia*, pages 5389–5397, 2022.

[26] Younghyun Jo, Seoung Wug Oh, Jaeyeon Kang, and Seon Joo Kim. Deep video super-resolution network using dynamic upsampling filters without explicit motion compensation. In *Proceedings of the IEEE conference on computer vision and pattern recognition*, pages 3224–3232, 2018.

[27] Diederik P Kingma and Jimmy Ba. Adam: A method for stochastic optimization. *arXiv preprint arXiv:1412.6980*, 2014.

[28] Huixia Li, Chenqian Yan, Shaohui Lin, Xiawu Zheng, Baochang Zhang, Fan Yang, and Rongrong Ji. Pams: Quantized super-resolution via parameterized max scale. In *Computer Vision–ECCV 2020: 16th European Conference, Glasgow, UK, August 23–28, 2020, Proceedings, Part XXV 16*, pages 564–580. Springer, 2020.

[29] Rundong Li, Yan Wang, Feng Liang, Hongwei Qin, Junjie Yan, and Rui Fan. Fully quantized network for object detection. In *Proceedings of the IEEE/CVF conference on computer vision and pattern recognition*, pages 2810–2819, 2019.

[30] Wenbo Li, Xin Tao, Taian Guo, Lu Qi, Jiangbo Lu, and Jiaya Jia. Mucan: Multi-correspondence aggregation network for video super-resolution. In *Computer Vision–ECCV 2020: 16th European Conference, Glasgow, UK, August 23–28, 2020, Proceedings, Part X 16*, pages 335–351. Springer, 2020.

[31] Wenjie Li, Juncheng Li, Guangwei Gao, Weihong Deng, Jiantao Zhou, Jian Yang, and Guo-Jun Qi. Cross-receptive focused inference network for lightweight image super-resolution. *IEEE Transactions on Multimedia*, 26:864–877, 2023.

[32] Wenjie Li, Heng Guo, Xuannan Liu, Kongming Liang, Jiani Hu, Zhanyu Ma, and Jun Guo. Efficient face super-resolution via wavelet-based feature enhancement network. In *Proceedings of the 32nd ACM International Conference on Multimedia*, pages 4515–4523, 2024.

[33] Yuhang Li, Ruihao Gong, Xu Tan, Yang Yang, Peng Hu, Qi Zhang, Fengwei Yu, Wei Wang, and Shi Gu. Brecq: Pushing the limit of post-training quantization by block reconstruction. *arXiv preprint arXiv:2102.05426*, 2021.

[34] Zhikai Li, Junrui Xiao, Lianwei Yang, and Qingyi Gu. Repq-vit: Scale reparameterization for post-training quantization of vision transformers. In *Proceedings of the IEEE/CVF International Conference on Computer Vision*, pages 17227–17236, 2023.

[35] Jingyun Liang, Jiezhang Cao, Guolei Sun, Kai Zhang, Luc Van Gool, and Radu Timofte. Swinir: Image restoration using swin transformer. In *Proceedings of the IEEE/CVF international conference on computer vision*, pages 1833–1844, 2021.

[36] Bee Lim, Sanghyun Son, Heewon Kim, Seungjun Nah, and Kyoung Mu Lee. Enhanced deep residual networks for single image super-resolution. In *Proceedings of the IEEE conference on computer vision and pattern recognition workshops*, pages 136–144, 2017.

[37] Boyu Liu, Haoyu Huang, Linlin Yang, Yanjing Li, Guodong Guo, Xianbin Cao, and Baochang Zhang. Efficient low-bit quantization with adaptive scales for multi-task co-training. In *The Thirteenth International Conference on Learning Representations*.

[38] Ce Liu and Deqing Sun. On bayesian adaptive video super resolution. *IEEE transactions on pattern analysis and machine intelligence*, 36(2):346–360, 2013.

[39] Chunxu Liu, Guozhen Zhang, Rui Zhao, and Limin Wang. Sparse global matching for video frame interpolation with large motion. In *Proceedings of the IEEE/CVF Conference on Computer Vision and Pattern Recognition*, pages 19125–19134, 2024.

[40] Kai Liu, Haotong Qin, Yong Guo, Xin Yuan, Linghe Kong, Guihai Chen, and Yulun Zhang. 2dquant: Low-bit post-training quantization for image super-resolution. *Advances in Neural Information Processing Systems*, 37:71068–71084, 2024.

[41] Kai Liu, Dehui Wang, Zhiteng Li, Zheng Chen, Yong Guo, Wenbo Li, Linghe Kong, and Yulun Zhang. Condiquant: Condition number based low-bit quantization for image super-resolution. *arXiv preprint arXiv:2502.15478*, 2025.

[42] Yijiang Liu, Huanrui Yang, Zhen Dong, Kurt Keutzer, Li Du, and Shanghang Zhang. Noisyquant: Noisy bias-enhanced post-training activation quantization for vision transformers. In *Proceedings of the IEEE/CVF Conference on Computer Vision and Pattern Recognition*, pages 20321–20330, 2023.

[43] Zechun Liu, Kwang-Ting Cheng, Dong Huang, Eric P Xing, and Zhiqiang Shen. Nonuniform-to-uniform quantization: Towards accurate quantization via generalized straight-through estimation. In *Proceedings of the IEEE/CVF conference on computer vision and pattern recognition*, pages 4942–4952, 2022.

[44] Ziwei Liu, Raymond A Yeh, Xiaoou Tang, Yiming Liu, and Aseem Agarwala. Video frame synthesis using deep voxel flow. In *Proceedings of the IEEE international conference on computer vision*, pages 4463–4471, 2017.

[45] Ilya Loshchilov and Frank Hutter. Sgdr: Stochastic gradient descent with warm restarts. *arXiv preprint arXiv:1608.03983*, 2016.

[46] Liying Lu, Ruizheng Wu, Huaijia Lin, Jiangbo Lu, and Jiaya Jia. Video frame interpolation with transformer. In *Proceedings of the IEEE/CVF Conference on Computer Vision and Pattern Recognition*, pages 3532–3542, 2022.

[47] Yuexiao Ma, Huixia Li, Xiawu Zheng, Feng Ling, Xuefeng Xiao, Rui Wang, Shilei Wen, Fei Chao, and Rongrong Ji. Outlier-aware slicing for post-training quantization in vision transformer. In *Forty-first International Conference on Machine Learning*, 2024.

[48] Anish Mittal, Rajiv Soundararajan, and Alan C Bovik. Making a "completely blind" image quality analyzer. *IEEE Signal processing letters*, 20(3):209–212, 2012.

[49] Jaehyeon Moon, Dohyung Kim, Junyong Cheon, and Bumsub Ham. Instance-aware group quantization for vision transformers. In *Proceedings of the IEEE/CVF Conference on Computer Vision and Pattern Recognition*, pages 16132–16141, 2024.

[50] Simon Niklaus and Feng Liu. Context-aware synthesis for video frame interpolation. In *Proceedings of the IEEE conference on computer vision and pattern recognition*, pages 1701–1710, 2018.

[51] Jiancheng Pan, Qing Ma, and Cong Bai. Reducing semantic confusion: Scene-aware aggregation network for remote sensing cross-modal retrieval. In *Proceedings of the 2023 ACM International Conference on Multimedia Retrieval*, pages 398–406, 2023.

[52] Jiancheng Pan, Yanxing Liu, Xiao He, Long Peng, Jiahao Li, Yuze Sun, and Xiaomeng Huang. Enhance then search: An augmentation-search strategy with foundation models for cross-domain few-shot object detection. In *Proceedings of the Computer Vision and Pattern Recognition Conference*, pages 1548–1556, 2025.

[53] Junheum Park, Jintae Kim, and Chang-Su Kim. Biformer: Learning bilateral motion estimation via bilateral transformer for 4k video frame interpolation. In *Proceedings of the IEEE/CVF Conference on Computer Vision and Pattern Recognition*, pages 1568–1577, 2023.

[54] A Paszke. Pytorch: An imperative style, high-performance deep learning library. *arXiv preprint arXiv:1912.01703*, 2019.

[55] Long Peng, Yang Cao, Yuejin Sun, and Yang Wang. Lightweight adaptive feature de-drifting for compressed image classification. *IEEE Transactions on Multimedia*, 26:6424–6436, 2024.

[56] Long Peng, Wenbo Li, Jiaming Guo, Xin Di, Haoze Sun, Yong Li, Renjing Pei, Yang Wang, Yang Cao, and Zheng-Jun Zha. Unveiling hidden details: A raw data-enhanced paradigm for real-world super-resolution. *arXiv preprint arXiv:2411.10798*, 2024.

[57] Long Peng, Wenbo Li, Renjing Pei, Jingjing Ren, Jiaqi Xu, Yang Wang, Yang Cao, and Zheng-Jun Zha. Towards realistic data generation for real-world super-resolution. *arXiv preprint arXiv:2406.07255*, 2024.

[58] Long Peng, Xin Di, Zhanfeng Feng, Wenbo Li, Renjing Pei, Yang Wang, Xueyang Fu, Yang Cao, and Zheng-Jun Zha. Directing mamba to complex textures: An efficient texture-aware state space model for image restoration. *arXiv preprint arXiv:2501.16583*, 2025.

[59] Long Peng, Yang Wang, Xin Di, Xueyang Fu, Yang Cao, Zheng-Jun Zha, et al. Boosting image de-raining via central-surrounding synergistic convolution. In *Proceedings of the AAAI Conference on Artificial Intelligence*, volume 39, pages 6470–6478, 2025.

[60] Long Peng, Anran Wu, Wenbo Li, Peizhe Xia, Xueyuan Dai, Xinjie Zhang, Xin Di, Haoze Sun, Renjing Pei, Yang Wang, et al. Pixel to gaussian: Ultra-fast continuous super-resolution with 2d gaussian modeling. *arXiv preprint arXiv:2503.06617*, 2025.

[61] Haotong Qin, Yulun Zhang, Yifu Ding, Xianglong Liu, Martin Danelljan, Fisher Yu, et al. Quantsr: accurate low-bit quantization for efficient image super-resolution. *Advances in Neural Information Processing Systems*, 36:56838–56848, 2023.

[62] Shuwei Shi, Jinjin Gu, Liangbin Xie, Xintao Wang, Yujiu Yang, and Chao Dong. Rethinking alignment in video super-resolution transformers. *Advances in Neural Information Processing Systems*, 35:36081–36093, 2022.

[63] Xin Tao, Hongyun Gao, Renjie Liao, Jue Wang, and Jiaya Jia. Detail-revealing deep video super-resolution. In *Proceedings of the IEEE international conference on computer vision*, pages 4472–4480, 2017.

[64] Zhijun Tu, Jie Hu, Hanting Chen, and Yunhe Wang. Toward accurate post-training quantization for image super resolution. In *Proceedings of the IEEE/CVF Conference on Computer Vision and Pattern Recognition*, pages 5856–5865, 2023.

[65] Han Vanholder. Efficient inference with tensorrt. In *GPU Technology Conference*, volume 1, pages 1–24, 2016.

[66] Hai Wang, Xiaoyu Xiang, Yapeng Tian, Wenming Yang, and Qingmin Liao. Stdan: deformable attention network for space-time video super-resolution. *IEEE Transactions on Neural Networks and Learning Systems*, 2023.

[67] Xintao Wang, Kelvin CK Chan, Ke Yu, Chao Dong, and Chen Change Loy. Edvr: Video restoration with enhanced deformable convolutional networks. In *Proceedings of the IEEE/CVF conference on computer vision and pattern recognition workshops*, pages 0–0, 2019.

[68] Zhou Wang, Alan C Bovik, Hamid R Sheikh, and Eero P Simoncelli. Image quality assessment: from error visibility to structural similarity. *IEEE transactions on image processing*, 13(4): 600–612, 2004.

[69] Pingyu Wu, Kai Zhu, Yu Liu, Liming Zhao, Wei Zhai, Yang Cao, and Zheng-Jun Zha. Improved video vae for latent video diffusion model. In *Proceedings of the Computer Vision and Pattern Recognition Conference*, pages 18124–18133, 2025.

[70] Zhuguanyu Wu, Jiaxin Chen, Hanwen Zhong, Di Huang, and Yunhong Wang. Adalog: Post-training quantization for vision transformers with adaptive logarithm quantizer. In *European Conference on Computer Vision*, pages 411–427. Springer, 2024.

[71] Xiaoyu Xiang, Yapeng Tian, Yulun Zhang, Yun Fu, Jan P Allebach, and Chenliang Xu. Zooming slow-mo: Fast and accurate one-stage space-time video super-resolution. In *Proceedings of the IEEE/CVF conference on computer vision and pattern recognition*, pages 3370–3379, 2020.

[72] Gang Xu, Jun Xu, Zhen Li, Liang Wang, Xing Sun, and Ming-Ming Cheng. Temporal modulation network for controllable space-time video super-resolution. In *Proceedings of the IEEE/CVF conference on computer vision and pattern recognition*, pages 6388–6397, 2021.

[73] Kai Xu, Ziwei Yu, Xin Wang, Michael Bi Mi, and Angela Yao. Enhancing video super-resolution via implicit resampling-based alignment. In *Proceedings of the IEEE/CVF Conference on Computer Vision and Pattern Recognition*, pages 2546–2555, 2024.

[74] Tianfan Xue, Baian Chen, Jiajun Wu, Donglai Wei, and William T Freeman. Video enhancement with task-oriented flow. *International Journal of Computer Vision*, 127:1106–1125, 2019.

[75] Jian Yang, Dacheng Yin, Yizhou Zhou, Fengyun Rao, Wei Zhai, Yang Cao, and Zheng-Jun Zha. Mmar: Towards lossless multi-modal auto-regressive probabilistic modeling. In *Proceedings of the Computer Vision and Pattern Recognition Conference*, pages 7974–7985, 2025.

[76] Zhihang Yuan, Chenhao Xue, Yiqi Chen, Qiang Wu, and Guangyu Sun. Ptq4vit: Post-training quantization for vision transformers with twin uniform quantization. In *European conference on computer vision*, pages 191–207. Springer, 2022.

[77] Wei Zhai, Yang Cao, Jing Zhang, Haiyong Xie, Dacheng Tao, and Zheng-Jun Zha. On exploring multiplicity of primitives and attributes for texture recognition in the wild. *IEEE Transactions on Pattern Analysis and Machine Intelligence*, 46(1):403–420, 2023.

[78] Guozhen Zhang, Yuhan Zhu, Haonan Wang, Youxin Chen, Gangshan Wu, and Limin Wang. Extracting motion and appearance via inter-frame attention for efficient video frame interpolation. In *Proceedings of the IEEE/CVF Conference on Computer Vision and Pattern Recognition*, pages 5682–5692, 2023.

[79] Guozhen Zhang, Yuhan Zhu, Haonan Wang, Youxin Chen, Gangshan Wu, and Limin Wang. Extracting motion and appearance via inter-frame attention for efficient video frame interpolation. In *Proceedings of the IEEE/CVF Conference on Computer Vision and Pattern Recognition*, pages 5682–5692, 2023.

[80] Guozhen Zhang, Chuxnu Liu, Yutao Cui, Xiaotong Zhao, Kai Ma, and Limin Wang. Vfimamba: Video frame interpolation with state space models. *Advances in Neural Information Processing Systems*, 37:107225–107248, 2024.

[81] Richard Zhang, Phillip Isola, Alexei A Efros, Eli Shechtman, and Oliver Wang. The unreasonable effectiveness of deep features as a perceptual metric. In *Proceedings of the IEEE conference on computer vision and pattern recognition*, pages 586–595, 2018.

[82] Yulun Zhang, Haotong Qin, Zixiang Zhao, Xianglong Liu, Martin Danelljan, and Fisher Yu. Flexible residual binarization for image super-resolution. In *Forty-first International Conference on Machine Learning*, 2024.

[83] Yaozong Zheng, Bineng Zhong, Qihua Liang, Ning Li, and Shuxiang Song. Decoupled spatio-temporal consistency learning for self-supervised tracking. In *Proceedings of the AAAI Conference on Artificial Intelligence*, volume 39, pages 10635–10643, 2025.

[84] Yaozong Zheng, Bineng Zhong, Qihua Liang, Shengping Zhang, Guorong Li, Xianxian Li, and Rongrong Ji. Towards universal modal tracking with online dense temporal token learning. *IEEE Transactions on Pattern Analysis and Machine Intelligence*, 2025.

[85] Yunshan Zhong, Jiawei Hu, You Huang, Yuxin Zhang, and Rongrong Ji. Erq: Error reduction for post-training quantization of vision transformers. In *Forty-first International Conference on Machine Learning*, 2024.

[86] Zhihang Zhong, Gurunandan Krishnan, Xiao Sun, Yu Qiao, Sizhuo Ma, and Jian Wang. Clearer frames, anytime: Resolving velocity ambiguity in video frame interpolation. In *European Conference on Computer Vision*, pages 346–363. Springer, 2024.

[87] Chengcheng Zhou, Zongqing Lu, Linge Li, Qiangyu Yan, and Jing-Hao Xue. How video super-resolution and frame interpolation mutually benefit. In *Proceedings of the 29th ACM International Conference on Multimedia*, pages 5445–5453, 2021.

[88] Xingyu Zhou, Leheng Zhang, Xiaorui Zhao, Keze Wang, Leida Li, and Shuhang Gu. Video super-resolution transformer with masked inter&intra-frame attention. In *Proceedings of the IEEE/CVF Conference on Computer Vision and Pattern Recognition*, pages 25399–25408, 2024.

[89] Yuhan Zhu, Guozhen Zhang, Jing Tan, Gangshan Wu, and Limin Wang. Dual detrs for multi-label temporal action detection. In *Proceedings of the IEEE/CVF Conference on Computer Vision and Pattern Recognition*, pages 18559–18569, 2024.

NeurIPS Paper Checklist

1. **Claims**

   Question: Do the main claims made in the abstract and introduction accurately reflect the paper's contributions and scope?

   Answer: [Yes]

   Justification: The abstract and introduction provide a clear and concise summary of the paper's main contributions, including the proposed methodology, and experimental findings. The scope and limitations are also explicitly stated.

   Guidelines:

   - The answer NA means that the abstract and introduction do not include the claims made in the paper.
   - The abstract and/or introduction should clearly state the claims made, including the contributions made in the paper and important assumptions and limitations. A No or NA answer to this question will not be perceived well by the reviewers.
   - The claims made should match theoretical and experimental results, and reflect how much the results can be expected to generalize to other settings.
   - It is fine to include aspirational goals as motivation as long as it is clear that these goals are not attained by the paper.

2. **Limitations**

   Question: Does the paper discuss the limitations of the work performed by the authors?

   Answer: [Yes]

   Justification: The limitations of our work are explicitly discussed in Section 5 of the paper.

   Guidelines:

   - The answer NA means that the paper has no limitation while the answer No means that the paper has limitations, but those are not discussed in the paper.
   - The authors are encouraged to create a separate "Limitations" section in their paper.
   - The paper should point out any strong assumptions and how robust the results are to violations of these assumptions (e.g., independence assumptions, noiseless settings, model well-specification, asymptotic approximations only holding locally). The authors should reflect on how these assumptions might be violated in practice and what the implications would be.
   - The authors should reflect on the scope of the claims made, e.g., if the approach was only tested on a few datasets or with a few runs. In general, empirical results often depend on implicit assumptions, which should be articulated.
   - The authors should reflect on the factors that influence the performance of the approach. For example, a facial recognition algorithm may perform poorly when image resolution is low or images are taken in low lighting. Or a speech-to-text system might not be used reliably to provide closed captions for online lectures because it fails to handle technical jargon.
   - The authors should discuss the computational efficiency of the proposed algorithms and how they scale with dataset size.
   - If applicable, the authors should discuss possible limitations of their approach to address problems of privacy and fairness.
   - While the authors might fear that complete honesty about limitations might be used by reviewers as grounds for rejection, a worse outcome might be that reviewers discover limitations that aren't acknowledged in the paper. The authors should use their best judgment and recognize that individual actions in favor of transparency play an important role in developing norms that preserve the integrity of the community. Reviewers will be specifically instructed to not penalize honesty concerning limitations.

3. **Theory assumptions and proofs**

   Question: For each theoretical result, does the paper provide the full set of assumptions and a complete (and correct) proof?

   Answer: [NA]

Justification: This paper focuses on proposing a novel quantization framework for multi-frame video enhancement and validates its effectiveness through extensive experiments. It does not present any theoretical results or proofs, as the contributions are primarily empirical and methodological.

Guidelines:

- The answer NA means that the paper does not include theoretical results.
- All the theorems, formulas, and proofs in the paper should be numbered and cross-referenced.
- All assumptions should be clearly stated or referenced in the statement of any theorems.
- The proofs can either appear in the main paper or the supplemental material, but if they appear in the supplemental material, the authors are encouraged to provide a short proof sketch to provide intuition.
- Inversely, any informal proof provided in the core of the paper should be complemented by formal proofs provided in appendix or supplemental material.
- Theorems and Lemmas that the proof relies upon should be properly referenced.

4. **Experimental result reproducibility**

   Question: Does the paper fully disclose all the information needed to reproduce the main experimental results of the paper to the extent that it affects the main claims and/or conclusions of the paper (regardless of whether the code and data are provided or not)?

   Answer: [Yes]

   Justification: The paper provides all necessary details to reproduce the experimental results, including the architecture design, hyperparameter settings, and dataset preprocessing steps in Section X. Additionally, pseudocode and implementation details are included in Appendix Y to facilitate reproducibility.

   Guidelines:

   - The answer NA means that the paper does not include experiments.
   - If the paper includes experiments, a No answer to this question will not be perceived well by the reviewers: Making the paper reproducible is important, regardless of whether the code and data are provided or not.
   - If the contribution is a dataset and/or model, the authors should describe the steps taken to make their results reproducible or verifiable.
   - Depending on the contribution, reproducibility can be accomplished in various ways. For example, if the contribution is a novel architecture, describing the architecture fully might suffice, or if the contribution is a specific model and empirical evaluation, it may be necessary to either make it possible for others to replicate the model with the same dataset, or provide access to the model. In general. releasing code and data is often one good way to accomplish this, but reproducibility can also be provided via detailed instructions for how to replicate the results, access to a hosted model (e.g., in the case of a large language model), releasing of a model checkpoint, or other means that are appropriate to the research performed.
   - While NeurIPS does not require releasing code, the conference does require all submissions to provide some reasonable avenue for reproducibility, which may depend on the nature of the contribution. For example
     (a) If the contribution is primarily a new algorithm, the paper should make it clear how to reproduce that algorithm.
     (b) If the contribution is primarily a new model architecture, the paper should describe the architecture clearly and fully.
     (c) If the contribution is a new model (e.g., a large language model), then there should either be a way to access this model for reproducing the results or a way to reproduce the model (e.g., with an open-source dataset or instructions for how to construct the dataset).
     (d) We recognize that reproducibility may be tricky in some cases, in which case authors are welcome to describe the particular way they provide for reproducibility. In the case of closed-source models, it may be that access to the model is limited in some way (e.g., to registered users), but it should be possible for other researchers to have some path to reproducing or verifying the results.

5. **Open access to data and code**

Question: Does the paper provide open access to the data and code, with sufficient instructions to faithfully reproduce the main experimental results, as described in supplemental material?

Answer: [No]

Justification: We plan to release the code and data in the near future to ensure reproducibility and to meet the community's expectations for open research. Specific timelines and access details will be provided as soon as they are finalized.

Guidelines:

- The answer NA means that paper does not include experiments requiring code.
- Please see the NeurIPS code and data submission guidelines (https://nips.cc/public/guides/CodeSubmissionPolicy) for more details.
- While we encourage the release of code and data, we understand that this might not be possible, so "No" is an acceptable answer. Papers cannot be rejected simply for not including code, unless this is central to the contribution (e.g., for a new open-source benchmark).
- The instructions should contain the exact command and environment needed to run to reproduce the results. See the NeurIPS code and data submission guidelines (https://nips.cc/public/guides/CodeSubmissionPolicy) for more details.
- The authors should provide instructions on data access and preparation, including how to access the raw data, preprocessed data, intermediate data, and generated data, etc.
- The authors should provide scripts to reproduce all experimental results for the new proposed method and baselines. If only a subset of experiments are reproducible, they should state which ones are omitted from the script and why.
- At submission time, to preserve anonymity, the authors should release anonymized versions (if applicable).
- Providing as much information as possible in supplemental material (appended to the paper) is recommended, but including URLs to data and code is permitted.

6. **Experimental setting/details**

Question: Does the paper specify all the training and test details (e.g., data splits, hyperparameters, how they were chosen, type of optimizer, etc.) necessary to understand the results?

Answer: [Yes]

Justification: The paper provides a comprehensive description of the experimental setup, including details on data splits, hyperparameters (e.g., learning rate, batch size), and the choice of optimizer.

Guidelines:

- The answer NA means that the paper does not include experiments.
- The experimental setting should be presented in the core of the paper to a level of detail that is necessary to appreciate the results and make sense of them.
- The full details can be provided either with the code, in appendix, or as supplemental material.

7. **Experiment statistical significance**

Question: Does the paper report error bars suitably and correctly defined or other appropriate information about the statistical significance of the experiments?

Answer: [No]

Justification: The paper currently does not include detailed error bars or statistical significance tests for the experiments. However, we plan to provide this information in future revisions

Guidelines:

- The answer NA means that the paper does not include experiments.
- The authors should answer "Yes" if the results are accompanied by error bars, confidence intervals, or statistical significance tests, at least for the experiments that support the main claims of the paper.
- The factors of variability that the error bars are capturing should be clearly stated (for example, train/test split, initialization, random drawing of some parameter, or overall run with given experimental conditions).
- The method for calculating the error bars should be explained (closed form formula, call to a library function, bootstrap, etc.)

- The assumptions made should be given (e.g., Normally distributed errors).
- It should be clear whether the error bar is the standard deviation or the standard error of the mean.
- It is OK to report 1-sigma error bars, but one should state it. The authors should preferably report a 2-sigma error bar than state that they have a 96% CI, if the hypothesis of Normality of errors is not verified.
- For asymmetric distributions, the authors should be careful not to show in tables or figures symmetric error bars that would yield results that are out of range (e.g. negative error rates).
- If error bars are reported in tables or plots, The authors should explain in the text how they were calculated and reference the corresponding figures or tables in the text.

8. **Experiments compute resources**

   Question: For each experiment, does the paper provide sufficient information on the computer resources (type of compute workers, memory, time of execution) needed to reproduce the experiments?

   Answer: [Yes]

   Justification: The paper provides detailed information on the compute resources used for the experiments.

   Guidelines:

   - The answer NA means that the paper does not include experiments.
   - The paper should indicate the type of compute workers CPU or GPU, internal cluster, or cloud provider, including relevant memory and storage.
   - The paper should provide the amount of compute required for each of the individual experimental runs as well as estimate the total compute.
   - The paper should disclose whether the full research project required more compute than the experiments reported in the paper (e.g., preliminary or failed experiments that didn't make it into the paper).

9. **Code of ethics**

   Question: Does the research conducted in the paper conform, in every respect, with the NeurIPS Code of Ethics https://neurips.cc/public/EthicsGuidelines?

   Answer: [Yes]

   Justification: The research complies fully with the NeurIPS Code of Ethics. All experiments were conducted responsibly, adhering to ethical guidelines, and no ethical concerns were identified.

   Guidelines:

   - The answer NA means that the authors have not reviewed the NeurIPS Code of Ethics.
   - If the authors answer No, they should explain the special circumstances that require a deviation from the Code of Ethics.
   - The authors should make sure to preserve anonymity (e.g., if there is a special consideration due to laws or regulations in their jurisdiction).

10. **Broader impacts**

    Question: Does the paper discuss both potential positive societal impacts and negative societal impacts of the work performed?

    Answer: [Yes]

    Justification: The research has the potential to advance the field of model quantization.

    Guidelines:

    - The answer NA means that there is no societal impact of the work performed.
    - If the authors answer NA or No, they should explain why their work has no societal impact or why the paper does not address societal impact.
    - Examples of negative societal impacts include potential malicious or unintended uses (e.g., disinformation, generating fake profiles, surveillance), fairness considerations (e.g., deployment of technologies that could make decisions that unfairly impact specific groups), privacy considerations, and security considerations.

- The conference expects that many papers will be foundational research and not tied to particular applications, let alone deployments. However, if there is a direct path to any negative applications, the authors should point it out. For example, it is legitimate to point out that an improvement in the quality of generative models could be used to generate deepfakes for disinformation. On the other hand, it is not needed to point out that a generic algorithm for optimizing neural networks could enable people to train models that generate Deepfakes faster.
- The authors should consider possible harms that could arise when the technology is being used as intended and functioning correctly, harms that could arise when the technology is being used as intended but gives incorrect results, and harms following from (intentional or unintentional) misuse of the technology.
- If there are negative societal impacts, the authors could also discuss possible mitigation strategies (e.g., gated release of models, providing defenses in addition to attacks, mechanisms for monitoring misuse, mechanisms to monitor how a system learns from feedback over time, improving the efficiency and accessibility of ML).

11. **Safeguards**

    Question: Does the paper describe safeguards that have been put in place for responsible release of data or models that have a high risk for misuse (e.g., pretrained language models, image generators, or scraped datasets)?

    Answer: [NA]

    Justification: The paper poses no such risks.

    Guidelines:

    - The answer NA means that the paper poses no such risks.
    - Released models that have a high risk for misuse or dual-use should be released with necessary safeguards to allow for controlled use of the model, for example by requiring that users adhere to usage guidelines or restrictions to access the model or implementing safety filters.
    - Datasets that have been scraped from the Internet could pose safety risks. The authors should describe how they avoided releasing unsafe images.
    - We recognize that providing effective safeguards is challenging, and many papers do not require this, but we encourage authors to take this into account and make a best faith effort.

12. **Licenses for existing assets**

    Question: Are the creators or original owners of assets (e.g., code, data, models), used in the paper, properly credited and are the license and terms of use explicitly mentioned and properly respected?

    Answer: [Yes]

    Justification: All external assets used in this paper (e.g., datasets, code, models) are properly credited and cited.

    Guidelines:

    - The answer NA means that the paper does not use existing assets.
    - The authors should cite the original paper that produced the code package or dataset.
    - The authors should state which version of the asset is used and, if possible, include a URL.
    - The name of the license (e.g., CC-BY 4.0) should be included for each asset.
    - For scraped data from a particular source (e.g., website), the copyright and terms of service of that source should be provided.
    - If assets are released, the license, copyright information, and terms of use in the package should be provided. For popular datasets, `paperswithcode.com/datasets` has curated licenses for some datasets. Their licensing guide can help determine the license of a dataset.
    - For existing datasets that are re-packaged, both the original license and the license of the derived asset (if it has changed) should be provided.
    - If this information is not available online, the authors are encouraged to reach out to the asset's creators.

13. **New assets**

    Question: Are new assets introduced in the paper well documented and is the documentation provided alongside the assets?

Answer: [NA]

Justification: The paper does not introduce any new assets.

Guidelines:

- The answer NA means that the paper does not release new assets.
- Researchers should communicate the details of the dataset/code/model as part of their submissions via structured templates. This includes details about training, license, limitations, etc.
- The paper should discuss whether and how consent was obtained from people whose asset is used.
- At submission time, remember to anonymize your assets (if applicable). You can either create an anonymized URL or include an anonymized zip file.

14. **Crowdsourcing and research with human subjects**

Question: For crowdsourcing experiments and research with human subjects, does the paper include the full text of instructions given to participants and screenshots, if applicable, as well as details about compensation (if any)?

Answer: [NA]

Justification: The paper does not involve crowdsourcing experiments or research with human subjects.

Guidelines:

- The answer NA means that the paper does not involve crowdsourcing nor research with human subjects.
- Including this information in the supplemental material is fine, but if the main contribution of the paper involves human subjects, then as much detail as possible should be included in the main paper.
- According to the NeurIPS Code of Ethics, workers involved in data collection, curation, or other labor should be paid at least the minimum wage in the country of the data collector.

15. **Institutional review board (IRB) approvals or equivalent for research with human subjects**

Question: Does the paper describe potential risks incurred by study participants, whether such risks were disclosed to the subjects, and whether Institutional Review Board (IRB) approvals (or an equivalent approval/review based on the requirements of your country or institution) were obtained?

Answer: [No]

Justification: The paper does not involve research with human subjects or crowdsourcing experiments, and therefore, IRB approval is not applicable.

Guidelines:

- The answer NA means that the paper does not involve crowdsourcing nor research with human subjects.
- Depending on the country in which research is conducted, IRB approval (or equivalent) may be required for any human subjects research. If you obtained IRB approval, you should clearly state this in the paper.
- We recognize that the procedures for this may vary significantly between institutions and locations, and we expect authors to adhere to the NeurIPS Code of Ethics and the guidelines for their institution.
- For initial submissions, do not include any information that would break anonymity (if applicable), such as the institution conducting the review.

16. **Declaration of LLM usage**

Question: Does the paper describe the usage of LLMs if it is an important, original, or non-standard component of the core methods in this research? Note that if the LLM is used only for writing, editing, or formatting purposes and does not impact the core methodology, scientific rigorousness, or originality of the research, declaration is not required.

Answer: [No]

Justification: The LLM was only used for editing grammar and formatting, which does not impact the scientific rigor or originality of the research.

Guidelines:

- The answer NA means that the core method development in this research does not involve LLMs as any important, original, or non-standard components.
- Please refer to our LLM policy (https://neurips.cc/Conferences/2025/LLM) for what should or should not be described.

Appendix / Supplemental material

A More Details about Quantization Scheme

This section provides further elaboration on the quantization process introduced in the problem formulation. We detail the quantization strategy employed for Transformer-based architectures and describe how gradient approximation is performed using the Straight-Through Estimator (STE), enabling end-to-end training under quantized constraints.

A.1 Quantization Strategy for Transformer Blocks

Following prior work [40, 42], we apply quantization to the most computationally intensive components of Transformer models, including all linear transformations and batched matrix multiplications. To simulate quantization during training, we adopt a fake quantization approach, wherein both weights and activations are quantized using floating-point operations that emulate integer arithmetic. Figure 5 illustrates the quantization workflow within a typical Transformer block, covering the QKV attention mechanism, Multi-Head Self-Attention (MSA), and the feed-forward network (MLP). All Q-Linear layers operate on quantized weights and activations [13, 14, 69, 75, 77, 83, 84], which are processed through dedicated quantizers prior to arithmetic operations. For simplicity, dropout layers in the attention and projection modules are omitted in the illustration.

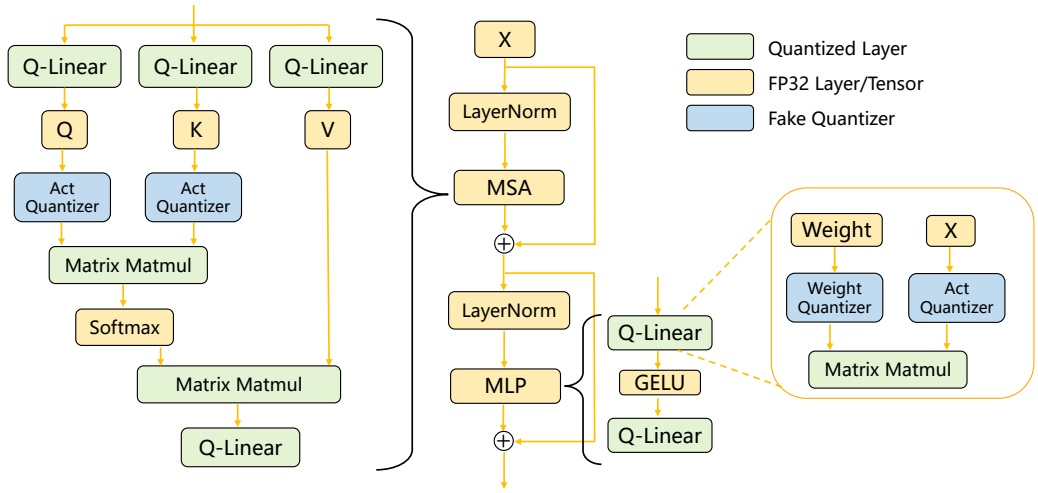

Figure 5: Quantization scheme for Transformer blocks. Green boxes denote quantized layers, yellow boxes indicate FP32 operations and tensors, and blue boxes represent fake quantizers. `Q-Linear` indicates a quantized linear transformation. Each matrix multiplication is performed on quantized weights and activations.

A.2 Gradient Approximation with STE

However, both the Clip and Round operations are non-differentiable, which impedes the use of gradient-based optimization methods [31, 32, 51, 52]. To overcome this, we adopt the Straight-Through Estimator (STE), where the gradients are approximated during backpropagation.

Specifically, for the Round operation, the gradient is approximated as:

$$\frac{\partial \text{Round}(x)}{\partial x} = 1. \tag{7}$$

For the Clip operation, the partial derivatives are approximated as:

$$\frac{\partial \text{Clip}(x, l, u)}{\partial x} = \begin{cases} 1, & \text{if} \quad l \leq x \leq u, \\ 0, & \text{otherwise}, \end{cases} \tag{8}$$

$$\frac{\partial \text{Clip}(x, l, u)}{\partial l} = \begin{cases} 1, & \text{if} \quad x < l, \\ 0, & \text{otherwise}, \end{cases} \quad \frac{\partial \text{Clip}(x, l, u)}{\partial u} = \begin{cases} 1, & \text{if} \quad x > u, \\ 0, & \text{otherwise}. \end{cases} \tag{9}$$

By leveraging these approximations, PTQ frameworks can fine-tune the clipping parameters $\{l_w, u_w\}$ for weights and $\{l_a, u_a\}$ for activations, enabling better adaptation to low-bit constraints without altering the original floating-point model parameters.

A.3 Distinguishing Our PTQ Approach from QAT

To prevent potential ambiguity, we explicitly define our methodology as **Post-Training Quantization (PTQ)**. A core principle of our approach is that throughout the entire quantization process, the weights of the pre-trained full-precision model are kept completely frozen and are never updated [11, 55, 57–60]. The optimization is exclusively aimed at determining the optimal quantization parameters, specifically the clipping bounds for both weights and activations.

A key aspect of our method is the use of fake quantization and the Straight-Through Estimator (STE) during the optimization of these clipping bounds. It is crucial to understand that these techniques are employed solely as a mechanism to enable gradient-based optimization of the clipping bounds through backpropagation. This strategy of optimizing quantization parameters while keeping weights fixed is a common and advanced technique in the PTQ literature, enabling more accurate parameter learning without the significant computational overhead of full model retraining [40, 76].

A.4 Clarification on Multi-Frame Quantization

We wish to clarify the term "multi-frame quantization" to accurately reflect its implementation and scope. The term does not imply that we store a unique set of quantization parameters for every single frame of an entire video sequence. Such an approach would be impractical, leading to prohibitive storage costs and failing to generalize to videos of arbitrary length.

Instead, our definition of multi-frame quantization is tailored to the operational architecture of modern video enhancement models. These models, whether based on sliding-window or recurrent structures, process a fixed number (N) of frames at each inference step. For instance, a sliding-window model takes a local window of N frames as input to produce an enhanced central frame.

Consequently, our "per-frame quantization" refers to the practice of learning and storing N distinct sets of clipping bounds—one for each of the N frame slots within this fixed-size processing window. This fine-grained approach captures local temporal dynamics more effectively, leading to superior quantization performance.

B More Details of Datasets and Training Settings.

In this work, we use the Vimeo-90K septuplet dataset [74] as the primary training dataset across all three tasks. The Vimeo-90K dataset contains 64,612 training clips and 7,824 testing clips, with each clip consisting of seven frames at a spatial resolution of 448×256. For evaluation, in addition to the Vimeo-90K test set, we also adopt the Vid4 dataset [38], a classical benchmark containing four video sequences (calendar, city, foliage, and walk). During the PTQ training phase, we adopt a knowledge distillation strategy where the supervision relies on teacher model predictions rather than HR references. However, the usage of the Vimeo-90K dataset slightly varies across tasks due to the differences in task requirements and experimental protocols, as detailed below.

For the STVSR task, we use the Vimeo-90K dataset [74] for training. each video clip in Vimeo-90K is treated as high-resolution (HR) and high-frame-rate (HFR) references. The low-resolution (LR) and low-frame-rate (LFR) inputs are generated by selecting odd-index frames from the HR sequences and downsampling them by a factor of 4 using bicubic interpolation. Following standard practices in previous STVSR studies [12, 66, 72], we evaluate the model on both the Vid4 dataset and the Vimeo-90K test set. The Vimeo-90K test set is further divided into Vimeo-Slow, Vimeo-Medium, and Vimeo-Fast subsets based on motion magnitude. To avoid infinite PSNR values, we exclude six sequences from the Vimeo-Medium subset and three from the Vimeo-Slow subset, as suggested in [66].

For the VSR task, we follow the experimental settings of prior works [5, 6, 62]. The Vimeo-90K dataset is used for training, with its seven-frame clips serving as training samples. For evaluation, we adopt both the Vimeo-90K test set (Vimeo90K-T) and the Vid4 dataset to benchmark model performance.

For the VFI task, we train our models on the Vimeo-90K septuplet dataset by following the experimental settings introduced in [88]. Two training paradigms are employed: (1) the **T** setting, which follows the traditional arbitrary time indexing paradigm where temporal interpolation is

performed at uniformly sampled time steps, and (2) the **D** setting, which adopts a distance-based indexing strategy, prioritizing frames closer to the input during interpolation. In line with [88], we use the first and last frames of each sequence as inputs to predict the intermediate five frames.

C Detailed Structure of Backbones.

C.1 Backbone for STVSR Task: RSTT

The Real-time Spatial Temporal Transformer (RSTT) [12] is a cascaded UNet-style architecture for joint temporal interpolation and spatial super-resolution. It consists of four encoder stages E_k and four corresponding decoder stages D_k $(k = 0, 1, 2, 3)$.

Given four consecutive low-resolution, low-frame-rate input frames $\{I^L_{2t-1}, I^L_{2t+1}, I^L_{2t+3}, I^L_{2t+5}\}$, the encoders extract multi-scale spatio-temporal features, which are stored as dictionaries. A query builder generates seven queries $\{Q_1, Q_2, \ldots, Q_7\}$ used to synthesize the target high-resolution, high-frame-rate frames via the decoder stages.

Encoder Block. Each encoder block consists of two sub-blocks: a Window-based Multi-head Self Attention (W-MSA) block and a Shifted Window-based Multi-head Self Attention (SW-MSA) block. Each sub-block is wrapped with Layer Normalization (LN), a multi-layer perceptron (MLP), and residual connections.

The computation in each encoder block is:

$$X = \text{W-MSA}(\text{LN}(X)) + X, \tag{10}$$
$$X = \text{MLP}(\text{LN}(X)) + X, \tag{11}$$
$$X = \text{SW-MSA}(\text{LN}(X)) + X, \tag{12}$$
$$X = \text{MLP}(\text{LN}(X)) + X. \tag{13}$$

For a windowed feature $X \in \mathbb{R}^{M^2 \times C}$, attention is computed as:

$$\text{Attention}(Q, K, V) = \text{Softmax}\left(\frac{QK^\top}{\sqrt{d}}\right)V, \quad Q = XW^Q,\ K = XW^K,\ V = XW^V. \tag{14}$$

Decoder Block. Each decoder block shares the same structure as the encoder block, except that self-attention is replaced by cross-attention. Specifically, W-MSA and SW-MSA are replaced by: Window-based Multi-head Cross Attention (W-MCA) and Shifted Window-based Multi-head Cross Attention (SW-MCA) The cross-attention is computed as:

$$\text{CrossAttention}(Q, K, V) = \text{Softmax}\left(\frac{QK^\top}{\sqrt{d}}\right)V. \tag{15}$$

In this case, the query Q comes from the decoder input (or previous output), while the key and value (K, V) are obtained from the encoder dictionaries at the corresponding level.

C.2 Backbone for VSR Task: MIA

The overall structure of MIA-VSR [88] follows the bi-directional second-order grid propagation framework as in BasicVSR++ [6]. The network consists of three main parts: feature extraction, feature propagation, and feature reconstruction. The **feature extraction** module uses convolution to extract shallow features from the input low-resolution (LR) frames. The **feature reconstruction** module adopts a pixel-shuffle layer to upsample and reconstruct the high-resolution (HR) frames. The core of the network lies in the middle: the **feature propagation module**, where the MIA blocks are applied to recurrently enhance features across frames. Each feature propagation module (FPM) consists of N cascaded Masked Inter&Intra-frame Attention Blocks (IIABs). For video frame t, the m-th FPM receives the current input $\boldsymbol{X}^t_m$ and the enhanced features from previous frames $\boldsymbol{X}^{t-1}_{m+1}, \boldsymbol{X}^{t-2}_{m+1}$ to produce the updated feature $\boldsymbol{X}^t_{m+1}$:

$$\boldsymbol{X}^t_{m+1} = \texttt{FPM}(\boldsymbol{X}^t_m, \boldsymbol{X}^{t-1}_{m+1}, \boldsymbol{X}^{t-2}_{m+1}). \tag{16}$$

Each block inside FPM performs the following update:

$$\boldsymbol{X}^t_{m,n+1} = \texttt{IIAB}(\boldsymbol{X}^t_{m,n}, \boldsymbol{X}^{t-1}_{m+1}, \boldsymbol{X}^{t-2}_{m+1}), \tag{17}$$

where $n = 0, \ldots, N-1$ and $\boldsymbol{X}^t_{m,0} = \boldsymbol{X}^t_m$. The attention mechanism is used inside each IIAB block. Instead of computing joint self-attention over concatenated features, MIA decouples attention into intra-frame and inter-frame branches. Specifically: The **Query** $\boldsymbol{Q}^t_{m,n}$ is generated only from the current feature $\boldsymbol{X}^t_{m,n}$. The **Keys** and **Values** contain both intra-frame tokens (from $\boldsymbol{X}^t_{m,n}$) and inter-frame tokens (from $\boldsymbol{X}^{t-1}_{m+1}, \boldsymbol{X}^{t-2}_{m+1}$). The QKV formulation in the IIAB block is as follows:

$$\begin{aligned} \boldsymbol{Q}^t_{m,n} &= \boldsymbol{X}^t_{m,n} W^Q, \\ \boldsymbol{K}^t_{m,n} &= \left[\boldsymbol{X}^t_{m,n} W^K; \left[\boldsymbol{X}^{t-1}_{m+1}; \boldsymbol{X}^{t-2}_{m+1}\right] W^K\right], \\ \boldsymbol{V}^t_{m,n} &= \left[\boldsymbol{X}^t_{m,n} W^V; \left[\boldsymbol{X}^{t-1}_{m+1}; \boldsymbol{X}^{t-2}_{m+1}\right] W^V\right], \end{aligned} \tag{18}$$

where W^Q, W^K, W^V are learnable projection matrices.

The attention output is computed as:

$$\texttt{Attn} = \text{Softmax}\left(\frac{\boldsymbol{Q}^t_{m,n} {\boldsymbol{K}^t_{m,n}}^\top}{\sqrt{d}} + B\right) \boldsymbol{V}^t_{m,n}, \tag{19}$$

where B is a learnable relative positional bias.

The output is then passed through a feedforward network (FFN) with LayerNorm and residual connections as in standard Transformer blocks.

C.3 Backbone for VFI Task: EMA-VFI

The overall architecture of EMA-VFI [78] consists of three main stages: (1) a CNN-based multi-scale feature extractor, (2) a Transformer-based motion-appearance feature extractor, and (3) a lightweight flow estimation module. The `FlowEstimation` module takes motion features $\boldsymbol{M}_{0\to1}$, $\boldsymbol{M}_{1\to0}$ and appearance features $\boldsymbol{A}_0$, $\boldsymbol{A}_1$ from the Transformer, and outputs refined flows $\boldsymbol{F}_{t\to0}$, $\boldsymbol{F}_{t\to1}$ along with a blending mask $\boldsymbol{O}_t$ to synthesize the intermediate frame.

Transformer Block. Each Transformer block is designed to jointly extract appearance and motion features using inter-frame attention. The block follows the standard Transformer layout with two residual sub-layers: an attention module and a feed-forward network (FFN):

$$\boldsymbol{X}' = \boldsymbol{X} + \texttt{InterFrameAttention}(\texttt{LN}(\boldsymbol{X})), \tag{20}$$

$$\boldsymbol{X}^{\text{out}} = \boldsymbol{X}' + \texttt{FFN}(\texttt{LN}(\boldsymbol{X}')), \tag{21}$$

where $\boldsymbol{X}$ is the input token feature derived from either I_0 or I_1.

Inter-frame Attention. The attention is computed between a patch in I_0 and its spatial neighbors in I_1, formulated as:

$$\boldsymbol{Q}_{i,j} = \boldsymbol{A}_0^{i,j} W^Q, \tag{22}$$

$$\boldsymbol{K}_{n(i,j)} = \boldsymbol{A}_1^{n(i,j)} W^K, \quad \boldsymbol{V}_{n(i,j)} = \boldsymbol{A}_1^{n(i,j)} W^V, \tag{23}$$

$$\boldsymbol{S}^{0\to1}_{i,j} = \text{Softmax}\left(\frac{\boldsymbol{Q}_{i,j} \cdot \boldsymbol{K}^\top_{n(i,j)}}{\sqrt{d}}\right), \tag{24}$$

where $n(i,j)$ denotes the spatial neighborhood around position (i,j).

Feed-forward Network (FFN). The FFN module incorporates depth-wise convolution to enhance spatial modeling:

$$\texttt{FFN}(\boldsymbol{X}) = \texttt{DWConv}(\texttt{GELU}(\boldsymbol{X} W_1)) W_2, \tag{25}$$

where `DWConv` denotes a depth-wise convolution operator.

The Transformer blocks are stacked to extract hierarchical motion and appearance features from multi-scale CNN features, providing rich spatiotemporal representations for accurate intermediate frame synthesis.

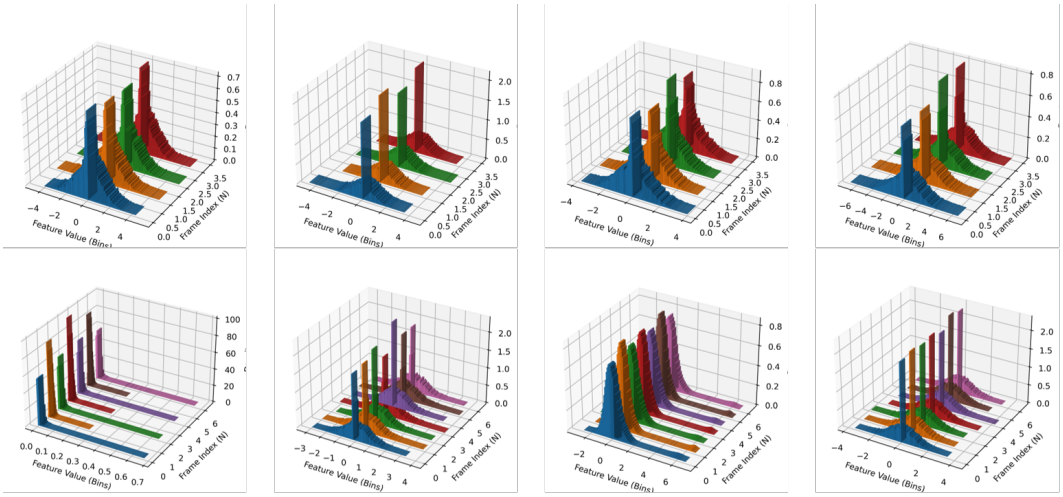

Figure 6: Per-frame activation statistics from Transformer layers. Each curve corresponds to a different frame in the input tensor.

Table 5: Quantitative comparison of different methods on four STVSR benchmarks under 6-bit quantization. The best and second best results are in **bold** and bold.

Method	Bit	Vid4		Vimeo-Fast		Vimeo-Medium		Vimeo-Slow	
		PSNR↑	SSIM↑	PSNR↑	SSIM↑	PSNR↑	SSIM↑	PSNR↑	SSIM↑
OpenVINO [15]	6/6	25.78	0.7692	35.49	0.9279	34.60	0.9259	32.67	0.8985
TensorRT [65]	6/6	25.71	0.7690	35.47	0.9275	34.60	0.9254	32.60	0.8981
SNPE [21]	6/6	25.92	0.7735	35.86	0.9315	34.71	0.9272	32.74	0.9035
Percentile [29]	6/6	25.88	0.7732	35.66	0.9298	34.64	0.9269	32.73	0.9035
MinMax [23]	6/6	25.96	0.7742	35.92	0.9315	34.69	0.9267	32.69	0.9021
NoisyQuant [42]	6/6	25.92	0.7741	35.81	0.9317	34.75	0.9281	32.70	0.9021
DBDC+Pac [64]	6/6	26.05	0.7837	36.10	0.9338	34.94	0.9303	32.92	0.9068
2DQuant [40]	6/6	26.04	0.7819	36.12	0.9339	34.95	0.9302	32.93	0.9068
Ours	6/6	**26.10**	**0.7850**	**36.21**	**0.9345**	**35.04**	**0.9311**	**33.00**	**0.9076**

D More Visualizations about Inter-frame Differences.

To further support the observation of frame-wise representational disparity discussed in Section 3.2, we present additional visualizations of activation distributions and attention patterns across frames in a multi-frame video enhancement model.

Figure 6 shows the per-frame activation value ranges collected from intermediate Transformer layers. We observe significant variation in both the minimum and maximum activation values across frames, indicating frame-dependent distribution shifts. The figure illustrates that the model dynamically attends to frames with varying intensity, further confirming that representational capacity is not uniformly allocated. These observations justify the need for frame-aware quantization strategies that account for inter-frame variation in activation statistics and attention dynamics.

E More Quantitative Results under additional bit-width

Table 5 presents the quantitative comparison of various quantization methods on four STVSR benchmarks under 6-bit quantization. As shown, our method consistently outperforms all existing approaches across all datasets in terms of both PSNR and SSIM.

F More Visual Comparisons

To further validate the visual effectiveness of our method, we present additional qualitative comparisons under 4-bit post-training quantization in Figure 7. The figure includes challenging examples from three representative video enhancement tasks: Space-Time Video Super-Resolution (STVSR), Video Super-Resolution (VSR), and Video Frame Interpolation (VFI).

As shown in the figure, traditional methods such as MinMax [23] and Percentile [29] often result in oversmoothed regions or noticeable artifacts. More advanced baselines like DBDC+Pac [64] and 2dquant [40] provide better structure but still suffer from detail loss, especially in textured or high-motion areas. In contrast, our method produces sharper edges and more faithful textures that are visually closer to the full-precision (FP) results.

These results further support the claim that our quantization approach better preserves perceptual quality across a wide range of scenes and motion patterns.

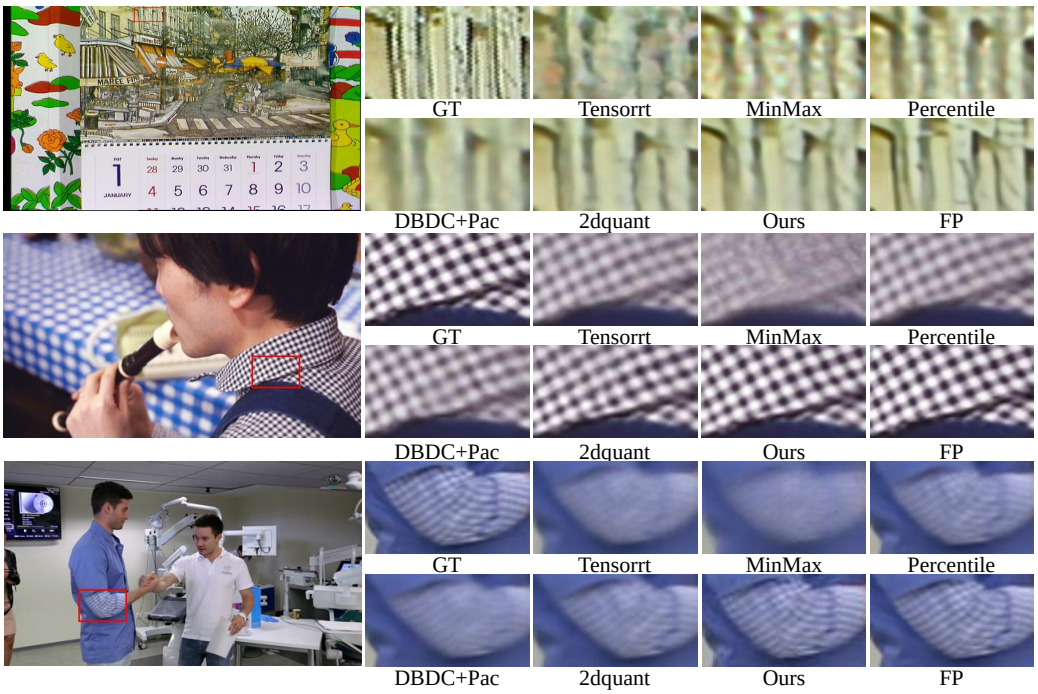

Figure 7: Additional visual comparisons under 4-bit quantization for three video enhancement tasks: STVSR, VSR, and VFI. Our method consistently produces outputs closer to the ground truth (GT) and full-precision (FP) results.

Table 6: Quantitative results under the 2-bit setting. PSNR and SSIM values are reported for multiple benchmark datasets. The best and the second best results are in **bold** and bold.

Method	Bit	Set5 (x2)		Set14 (x2)		B100 (x2)		Urban100 (x2)		Manga109 (x2)	
		PSNR↑	SSIM↑	PSNR↑	SSIM↑	PSNR↑	SSIM↑	PSNR↑	SSIM↑	PSNR↑	SSIM↑
SwinIR-light [35]	32	38.15	0.9611	33.86	0.9206	32.31	0.9012	32.76	0.9340	39.11	0.9781
Bicubic	32	32.25	0.9118	29.25	0.8406	28.68	0.8104	25.96	0.8088	29.17	0.9128
MinMax [23]	2	33.88	0.8951	30.05	0.8428	29.99	0.7232	26.30	0.7378	32.57	0.9446
Percentile [29]	2	34.35	0.9015	30.55	0.8466	30.45	0.7276	26.73	0.7464	33.10	0.9502
DBDC+Pac [64]	2	34.55	0.9052	30.65	0.8487	30.55	0.7291	26.85	0.7493	33.25	0.9529
DOBI [40]	2	35.25	0.9361	31.72	0.8917	30.62	0.8699	28.52	0.8727	33.65	0.9529
2DQuant [40]	2	36.00	0.9497	31.98	0.9012	30.91	0.8810	28.62	0.8819	34.40	0.9602
BTBI+PMTD	2	**36.07**	**0.9501**	**32.04**	**0.9014**	**31.00**	**0.8821**	**28.68**	**0.8905**	**34.45**	**0.9615**

G User Stduy

To evaluate the visual quality of the image super-resolution results, we conducted a user study involving 15 participants. Fifteen images were randomly selected from the test datasets, and the participants were asked to rate the quality of each processed image on a scale from 0 (poor quality) to 10 (excellent quality). The aggregated results, as illustrated in the figure, indicate that existing methods struggle to fully restore image quality, resulting in lower user satisfaction. In contrast, our method achieves the highest average score of 8.1, significantly outperforming other methods and demonstrating superior capabilities in visual performance and generalization.

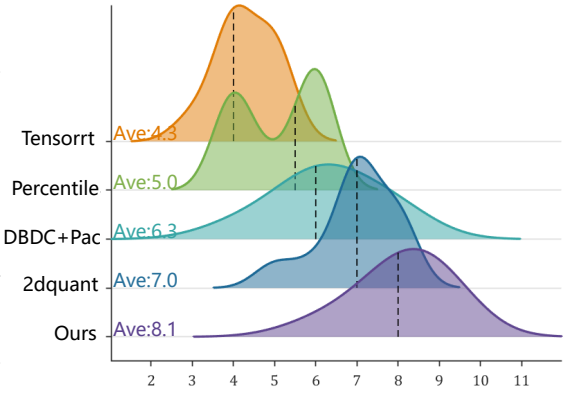

Figure 8: User study on image visual quality.

H More Ablation Studys

In this section, we provide additional ablation studies to verify the effectiveness of our proposed method. Specifically, we replace the core components of 2DQuant [40] with our approach. That is, we replace DOBI with BTBI and DQC with our multi-teacher distillation network. Following the experimental setup in 2DQuant, we conduct experiments under the 2-bit setting. The results demonstrate that our method achieves significant improvements over the baseline, as shown in Table 6.